

T.C.
DOKUZ EYLÜL UNIVERSITY
İZMİR INTERNATIONAL BIOMEDICINE AND GENOME
INSTITUTE

**DEVELOPMENT OF LYSOSOMAL ACID
LIPASE DEFICIENCY MODEL IN 3
DIMENSIONAL HEPATIC ORGANOIDS**

KÜBRA NUR KAPLAN İLHAN

DEPARTMENT OF MOLECULAR BIOLOGY AND
GENETICS

MASTER OF SCIENCE THESIS

İZMİR – 2019

TEZ KODU: DEU.IBG.MSc.2016850001

T.C.
DOKUZ EYLÜL UNIVERSITY
IZMIR INTERNATIONAL BIOMEDICINE AND GENOME
INSTITUTE

**DEVELOPMENT OF LYSOSOMAL ACID
LIPASE DEFICIENCY MODEL IN 3
DIMENSIONAL HEPATIC ORGANOIDS**

DEPARTMENT OF MOLECULAR BIOLOGY AND
GENETICS

MASTER OF SCIENCE THESIS

KÜBRA NUR KAPLAN İLHAN

Supervising Faculty Member: Prof. Dr. Esra ERDAL

TEZ KODU: DEU.IBG.MSc.2016850001

Dokuz Eylül Üniversitesi İzmir Uluslararası Biyotıp ve Genom Enstitüsü Genom Bilimleri ve Moleküler Biyoteknoloji Anabilim Dalı,
Moleküler Biyoloji ve Genetik Yüksek Lisans programı öğrencisi Kübra Nur Kaplan İlhan 'ÜÇ BOYUTLU HEPATİK ORGANOİDLERDE LİZOSOMAL ASİT LİPAZ EKSİKLİĞİ MODELİNİN GELİŞTİRİLMESİ' konulu Yüksek Lisans tezini 29/07/2019 tarihinde başarılı olarak tamamlamıştır.



Prof. Dr. Esra ERDAL
BAŞKAN



ÜYE
Prof. Dr. Hülya AYAR KAYALI



ÜYE
Doç. Dr. Buket KOSOVA

YEDEK ÜYE
Prof. Dr. Nur ARSLAN

YEDEK ÜYE
Prof. Dr. Devrim PESEN OKVUR

Dokuz Eylül University İzmir International Biomedicine and Genome Institute Department of
Genomics and Molecular Biotechnology,
Molecular Biology and Genetics graduate program Master of Science student Kübra Nur Kaplan
İlhan has successfully completed his Master of Science thesis titled '**DEVELOPMENT OF
LYSOSOMAL ACID LIPASE DEFICIENCY MODEL IN 3 DIMENSIONAL HEPATIC
ORGANOIDS**' on the date of 29/07/2019.



Prof. Dr. Esra ERDAL
CHAIR



MEMBER
Prof. Dr. Hülya AYAR KAYALI



MEMBER
Assoc. Prof. Buket KOSOVA

SUBSTITUTE MEMBER
Prof. Dr. Nur ARSLAN

SUBSTITUTE MEMBER
Prof. Dr. Devrim PESEN OKVUR

TABLE OF CONTENTS

LIST OF ABBREVIATIONS.....	ix
ACKNOWLEDGMENT.....	X
ABSTRACT.....	1
ÖZET.....	3
1.1. STATEMENT AND IMPORTANCE OF THE PROBLEM.....	5
1.2. AIM OF THE STUDY.....	5
1.3. THE HYPOTHESIS OF THE STUDY.....	5
2. GENERAL INFORMATION.....	6
2.1. LIVER & LIVER DISEASES.....	6
2.2. MODELING OF LIVER DISEASES.....	7
2.2.1. <i>Organoids for Disease Modelling</i>	8
2.2.1.1. <i>Liver Organoids</i>	8
2.3 WOLMAN AND CHOLESTEROL ESTER STORAGE DISEASES.....	9
2.3.1. <i>The Role of LAL Enzyme in Health and Disease</i>	10
2.3.2. <i>Established Models of LALD and Treatment Strategies</i>	13
3. MATERIALS AND METHOD.....	15
3.1 TYPE OF STUDY.....	15
3.2 TIME AND LOCATION OF STUDY.....	15
3.3 POPULATION AND SAMPLE OF STUDY.....	15
3.4 MATERIALS OF STUDY.....	15
3.5 VARIABLES OF THE STUDY.....	15
3.6. TOOLS FOR DATA COLLECTION.....	16
3.6.1. <i>Starting Material</i>	16
3.6.2. <i>Conditional Knock-Down of LIPA Gene in iPSCs</i>	16
3.6.2.1 <i>shLIPA and Non-Target Control Plasmid Preparation</i>	16
3.6.2.2 <i>Plasmid DNA Midiprep</i>	17
3.6.2.3 <i>Production of Lentiviral shRNA Constructs in Hek293T Cell Line</i>	17
3.6.3. <i>Generation of iPSC Derived Mature Hepatocytes</i>	18
3.6.4. <i>Generation of Endodermal Hepatic Organoids (eHEPOs)</i>	18
3.6.4.1. <i>Differentiation of iPSCs to Endoderm and Hepatic Progenitor Cells</i>	18
3.6.4.2. <i>Separation of EpCAM + Cells by FACS</i>	19
3.6.4.3. <i>Formation and Expansion of eHEPO Culture</i>	19
3.6.4.4. <i>Differentiation to Functional eHEPOs</i>	19
3.6.5. <i>Characterization of eHEPOs</i>	20
3.6.6. <i>LAL Enzyme Activity Determination</i>	22

3.6.7. <i>Materials Used</i>	23
3.7. STUDY PLAN AND CALENDAR	25
3.8. DATA EVALUATION	25
3.9. LIMITATIONS OF THE STUDY.....	25
3.10. ETHICS COMMITTEE APPROVAL	27
4. RESULTS	29
4.1. DEVELOPMENT OF 2D AND 3D HEPATOCYTE CULTURES FROM IPSCS	29
4.1.1. <i>Differentiation of IPSCs to Definitive Endoderm</i>	29
4.1.2. <i>Development of 2D Hepatocyte Culture from IPSCs</i>	30
4.1.3. <i>Development of 3D Endodermal Hepatic Organoid (eHEPO) Culture from IPSCs</i>	31
4.2. DETERMINATION OF LAL ENZYME ACTIVITY IN HEALTHY HEPATOCYTES AND eHEPOS	32
4.3. DETERMINATION OF OPTIMAL CONDITIONS FOR GENE SILENCING	33
4.4. CONDITIONAL KNOCK-DOWN OF LIPA GENE IN IPSCS	35
4.4.1. <i>Establishing LAL Deficient Stable IPSC Lines</i>	35
4.4.2. <i>Development of 2D Hepatocyte Culture from LAL Deficient IPSCs</i>	36
4.4.3. <i>Development of 3D Hepatocyte Culture from LAL Deficient IPSCs</i>	37
4.4. VERIFICATION OF 2D AND 3D LALD MODEL	38
5. DISCUSSION	41
6. CONCLUSION AND FUTURE ASPECTS	43
7. REFERENCES	44

Index of Figures

Figure 1: Main functions of the liver.....	6
Figure 2: Established Organoid Models and Their Cell of Origins.....	9
Figure 3: LAL enzyme working mechanism.....	11
Figure 4: Cholesterol metabolism in healthy and LAL deficient hepatocytes	12
Figure 5: The map of inducible lentiviral shRNA construct	17
Figure 6: Schematic representation of work-flow and representative BF images	29
Figure 7: Flow Cytometry analysis and Immune Fluorescence (IF) stainings of iPSC colonies and DE cells.....	30
Figure 8: Flow Cytometry analysis and Immune Fluorescent (IF) stainings of BP and MH cells and Albumin ELISA assay for the hepatocyte function.....	31
Figure 9: Organoid establishment and functionality tests	32
Figure 10: Schematic workflow of the enzyme activity assay and the LAL enzyme activity comparison between 2D hepatocytes and 3D hepatic organoids	33
Figure 11: Workflow of the shRNA silencing in Huh-7 cell line and LIPA expression levels after shRNA expression determined via quantitative real-time PCR.....	34
Figure 12: Basal LIPA expression levels in Huh-7, iPSC and HepG2 determined via quantitative real-time PCR.	35
Figure 13: Workflow of the shRNA silencing in iPSC colonies and LIPA expression levels after shRNA expression determined via quantitative real-time PCR.	36
Figure 14: BF images of differentiated iPSC colonies	37
Figure 15: FACS gating percentage for the EpCAM+/GFP+ cell population and BF images of EM and DM eHEPOs.	37
Figure 16: LIPA gene expression levels of differentiated 2D and 3D hepatocytes and determination of specific activity of the LAL enzyme.....	38
Figure 17: Albumin secretion levels of 2D and 3D models are determined by ELISA.	39
Figure 18: Immunofluorescent staining of 2D and 3D hepatocytes (MDH: lipid, PI: nucleus)	40

Index of Tables

Table 1: shRNA sequences and product numbers	16
Table 2: cDNA synthesis reaction set up.....	20
Table 3: Quantitative real-time PCR reaction set up with SYBR Green reagent.....	21
Table 4: Primer Sequences and T _m values.....	21
Table 5: Materials with catalog numbers	24
Table 6: Equipment list	24



LIST OF ABBREVIATIONS

2D	Two-Dimensional
3D	Three-Dimensional
AA	Amino acid
aSC	Adult Stem Cell
CE	Cholesterol Ester
CESD	Cholesterol Ester Storage Disease
CM	Conditioned Medium
DM	Differentiation Medium
EM	Expansion Medium
ESC	Embryonic Stem Cell
FA	Fatty Acid
FAB-1	Fatty Acid Binding Protein-1
FACS	Fluorescence Activated Cell Sorting
FC	Free Cholesterol
IF	Immune Fluorescent
IPSC	Induced Pluripotent Stem Cell
LAL	Lysosomal Acid Lipase
LALD	Lysosomal Acid Lipase Deficiency
LD	Lipid Droplet
LDL	Low-Density Lipoprotein
M6P	Mannose-6-Phosphate
NTC	Non-Target Control
PSC	Pluripotent Stem Cell
RSPO-1	Rspondin-1
shRNA	Small Hairpin RNA
WD	Wolman Disease

Acknowledgment

First of all, I would like to thank my thesis advisor, Prof. Dr. Esra ERDAL for giving me this chance to work with her and her wise guidance, for her support whenever I doubt myself and for believing in me. I am grateful for this experience, for this journey we took with all my lab mates.

I also would like to thank Soheil Akbari, whom without this experience would be not as easy and fruitful. He has always listened to my endless questions and concerns about my experimental designs and results. He has always guided me just enough so that I will learn to answer my own questions in time. He has taught me a lot; I will always be grateful.

İbrahim İlhan, my beloved and very patient husband, without your support and constant nudging, when I want to give up; I would not have done it. Thank you for always being on the other end of the phone whenever I needed it. Thank you for always putting my needs and problems before anything else and running here to help me get back on my feet whenever I felt like I couldn't. I am also very grateful to my family for being always there for me. My mom who has spent long boring days at my home in İzmir just to keep me fed and rested when I needed some company. My dad, who has supported me to come here, even though he hated to send his child away from his sight. Thank you for everything. My sister who has been a friend to me always, I am sorry for not being with you when you needed me the most and thank you, for understanding this, for your unconditional love. And finally, my very ambitious aunt, Aynur Kaplan, I have not been here without your constant support for me to be the best version of myself. I will always be grateful for what you have done for me.

My friends who we have spent many long days, Meltem Altunay, İrem Şimşek, Olcay Burçin Akbulud, and Deniz Kurşun, we have shared so many good and bad memories. Before anything else, I would like to thank you for your patience with me, for always tolerating me even though I was late always and late by an hour. For sharing your weekends with me, for keeping me company even when I am at my worst and all unbearable. After all the coffee we have had together, we shall be in debt to always remember each other, and blame one another for the addiction and insomnia. Still, you made it more bearable, I will miss you greatly.

Also, I would like to thank my lab mates we have spent many good and not so good days, but your friendship and help have made life easier. Mustafa, special thanks for patiently helping out to me when I was just a new, impatient member of this lab and needed help for so many basic things. Bilge, always stay positive! There were days, without you I would have drowned. I am very grateful for your understanding and loving nature, and for your efforts to keep me positive and sane.

And last but not the least, special thanks to AYAR-KAYALI LAB, Prof. Dr. Hülya Ayar Kayalı for opening her lab for enzyme activity experiments and helping us with the idea. And I would also like to thank Elçin Çağatay, Seminay Güler and Gizem Kurşunluoğlu for performing the enzyme activity assay. I am so grateful for your time and efforts.

“So long, and thank you for all the fish!”

DEVELOPMENT OF LYSOSOMAL ACID LIPASE DEFICIENCY MODEL IN 3 DIMENSIONAL HEPATIC ORGANOIDS

Kübra Nur Kaplan İlhan, İzmir International Biomedicine and Genome Institute, Dokuz Eylül
University Health Campus, Balçova, 35340, İzmir / Turkey

ABSTRACT

In the last decade, organoids have become the most powerful cell culture tool to study human biology in health and disease. Organoids are three-dimensional structures grown in an extracellular matrix that resemble organ structure and show organ-specific functions. Recently established protocols for liver-specific organoids enables the understanding of disease pathology and improvement of patient-specific therapies. Our aim in this work is to utilize organoid technology to model Lysosomal acid lipase deficiency (LALD).

Lysosomal acid lipase (LAL) is an enzyme, mainly found in the liver, that breaks down cholesterol esters into free cholesterol. In the absence of the LAL enzyme, cholesterol esters begin to accumulate in liver cells and a spectrum of symptoms can be observed. The mild form with 3%-5% enzyme activity is called cholesterol ester storage disease (CESD) and it can go undiagnosed for years but the severe form is Wolman's disease with less than 1% LAL enzyme activity. Unless treated, WD patients have a life span of maximum a year. LALD models are limited to animal models. These models are completely inadequate when a personalized approach is desired to be developed. Until recently, there were no cell lines that model LALD, however, a recent study has established Wolman Disease organoids from patient-derived iPSCs and thus, paved the way for the understanding of molecular mechanism and treatment options for the disease. In this thesis, first, we have established iPSC clones stably expressing an inducible shRNA vector for the LIPA gene, then we have created an iPSC derived 2D hepatocyte and 3D endodermal hepatic organoid (eHEPO) model for the LALD. LAL deficient 2D hepatocytes have shown to have decreased levels of LAL enzyme activity in comparison with healthy counterparts. On the contrary, our eHEPO model has not been successful to show LAL enzyme activity impairment after a 40% reduction in gene expression. Thus, we conclude that a more dramatic decrease in the gene expression level is needed to mimic the disease phenotype. This suggests that strict regulation of the enzyme activity is present in the 3D organoid model and further

investigation of molecular changes and regulation pathways is needed to understand the disease mechanism.

Keywords: Hepatic organoid, LIPA, LAL, Lysosomal Acid Lipase Deficiency, Wolman Disease, Cholesterol Ester Storage Disease, Disease Modelling



ÜÇ BOYUTLU HEPATİK ORGANOİDLERDE LİZOZOMAL ASİT LİPAZ EKSİKLİĞİ MODELİNİN GELİŞTİRİLMESİ

Kübra Nur Kaplan İlhan, İzmir Uluslararası Biyotıp ve Genom Enstitüsü, Dokuz Eylül
Universitesi, Sağlık Kampüsü, Balçova, 35340, İzmir / Turkey

ÖZET

Son zamanlarda, organoidler sağlık ve hastalıkta insan biyolojisini incelemek için oldukça güçlü bir hücre kültürü yöntemi haline gelmiştir. Organoidler, ekstraselüler matriste büyütülen, organın yapısını ve fonksiyonlarını gösteren üç boyutlu yapılardır. Son zamanlarda karaciğere özgü organoidler için yayınlanmış protokoller hastalık patolojisinin anlaşılmasını ve hastaya özgü tedavilerin geliştirilmesini sağlamakta yeni bir dönemin açılmasını sağlamıştır. Bu çalışmada amacımız Lizozomal asit lipaz eksikliği (LALD) için bir model geliştirmektir.

Lizozomal asit lipaz (LAL), çoğunlukla olarak karaciğerde bulunan ve kolesterol esterlerini serbest kolesterole parçalayan bir enzimdir. LAL enziminin yokluğunda, karaciğer hücrelerinde kolesterol esterleri birikmeye başlar ve çeşitli şiddetlerde lizozomal asit lipaz eksikliği patolojileri gözlenebilir. LALD spektrumunun en şiddetli formu, Wolman hastalığıdır ve maksimum % 1 LAL aktivitesi olan bu hastalar çoğunlukla hayatlarının ilk bir yılı içinde hayatlarını kaybetmektedir. Bununla birlikte, kolesterol ester depo hastalığı, % 3 ila % 5 enzim aktivitesine sahip daha hafif formları isimlendirmek için kullanılır. Bu hastalar, teşhis dahi konmadan erişkinliği boyunca yaşayabilen ve ancak yetişkin yaşlarda bazı semptomlar göstermektedir.

Lizozomal asit lipaz eksikliği modelleri şu ana kadar hayvan modelleriyle sınırlıdır ve kişiselleştirilmiş bir yaklaşım geliştirilmek istendiğinde bu modeller oldukça yetersizdir. Yakın zamana kadar, LALD'yi modelleyen hücre hatları ya da modelleri bulunmamaktaydı, ancak yakın zamanda yapılan bir çalışmada hasta kaynaklı uPKH'lerden Wolman Hastalığı organoidleri oluşturulmuş ve böylece hastalık için moleküler mekanizma ve tedavi seçeneklerinin anlaşılmasının önü açılmıştır. Bu tez çalışmasında öncelikle, LIPA geni için indüklenebilir bir shRNA vektörünü kalıcı olarak eksprese eden uPKH klonları oluşturulmuş,

daha sonra LALD için bir uPKH kaynaklı endodermal hepatik organoid (eHEPO) modeli ve 2 boyutlu (2B) hepatosit modeli yapılmıştır. LAL eksikliği olan 2B hepatositlerin, sağlıklı olanlara kıyasla LAL enzim aktivitesi seviyelerinde azalma gösterilmiştir. Ancak, eHEPO modelimizde, LIPA gen ekspresyonunda % 40'lık bir düşüşün ardından LAL enzim aktivitesinde düşüş gözlenmemiştir. Bu nedenle, hastalık fenotipini taklit etmek için gen ekspresyon seviyesinde daha dramatik bir düşüşün gerekli olduğu ve bunun sebebinin 3B organoid modelinde enzim aktivitesinin daha sıkı bir şekilde düzenlenmesinin neden olabileceği sonucuna varılmıştır. Bu durum, hastalık mekanizmasını anlamak için moleküler değişikliklerin ve enzim aktivitesini düzenleyen yolların daha detaylı araştırılması gerektiğini göstermektedir.

Anahtar Sözcükler: Hepatik Organoid, LIPA, LAL, Lizozomal Asit Lipaz Eksikliği, Wolman Hastalığı, Kolesterol Ester Depo Hastalığı

1. INTRODUCTION AND AIM

1.1. Statement and Importance of the Problem

Dysregulation of the enzymatic activity of Lysosomal Acid Lipase (LAL) causes a spectrum of LAL diseases ranging from Wolman Disease (WD) with complete inactivation to Cholesterol Ester Storage Disease (CESD) with partially absent. WD is diagnosed usually in the first few weeks of the patients' life and their life expectancy is at most a year without treatment. However, in 2015 a recombinant lysosomal acid lipase named sebalipase alpha is approved for the treatment of Wolman Disease and so far it is the only reliable treatment option. During the drug development process animal models of the disease had been established and used but there was no in-vitro model of the disease until recently. Although animal testing is widely accepted and also necessary to investigate drug efficiency and safety, there are, inevitably, several drawbacks of it: First of all animal models do not reflect human disease pathology reliably. Secondly, differences among species result in different outcomes of the same agent. Also, most animal experiments are done with the minimum number of animals without performing power analysis, therefore the results of these studies not always come out to be significant, and another major problem is the cost of animal testing especially when dealing with high throughput experimental designs.

1.2. Aim of the Study

We propose that there is a need to obtain reliable and adjustable *in vitro* models to investigate the molecular mechanism of the disease and to have a cheaper, robust and long-term model for deciding the dosage and effect of the current drug/candidate drugs. **As an effort to satisfy this need, we have proposed to develop 2D and 3D hepatocyte culture model of LALD.**

1.3. The hypothesis of the Study

We hypothesize that LIPA gene expression and consequently, LAL enzyme activity can be altered using an inducible lentiviral vector system on 2D mature hepatocyte and/or 3D hepatic organoids differentiated from healthy inducible pluripotent stem cells (hiPSCs).

2. GENERAL INFORMATION

2.1. Liver & Liver Diseases

The liver is one of the most critical organs due to its complex and integrated roles within the body (Figure 1). Blood detoxification, glucose, urea and fat metabolism, production of serum proteins and some hormones are some of those which places the liver in a central position for the protection of homeostasis in the body (Gordillo et. al. , 2015). These activities are carried out by harmonized studies of various cells such as hepatocytes, cholangiocytes, endothelial and stellate cells (Berasain and Avila 2015), but since the liver is predominantly (80%) composed of hepatocytes, they are frequently used in drug discovery and toxicology studies without any other non-parenchymal cells (Kostadinova et al. 2013).

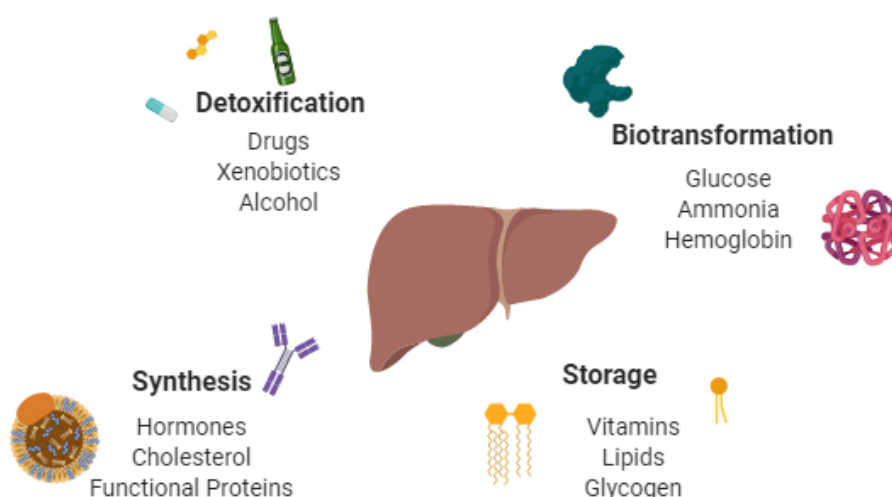


Figure 1: Main functions of the liver

Liver is the main organ for the regulation of body homeostasis through the detoxification and biotransformation of toxic substances and, synthesis, and storage of various monomers and their complex products

The prevalence of liver diseases is rising and causes approximately 2 million deaths per year worldwide (Asrani, Devarbhavi, Eaton, & Kamath, 2019). The etiologies of chronic liver diseases are multifactorial, ranging from familial history/inheritance to life-style and geographical conditions. Chronic viral infections (hepatitis B and C), excessive alcohol consumption, obesity-related fatty liver disease, and steatohepatitis, inherited diseases

(Wilson's disease, storage disorders, hepatorenal tyrosinemia, etc.) or autoimmune liver diseases are some of the liver-related diseases (Zhou, Zhang, & Qiao, 2014). Although a variety of therapies are available to treat patients suffering from liver diseases with different etiologies, liver transplantation is unfortunately only the curative option for the end-stage liver disease so far. Until now, the hepatocyte transplantation is the most promising alternative for treatment, however, a successful method for the long term culture of functional hepatocytes is not available yet. Thus, there is a major need to develop new treatment strategies for liver diseases.

2.2. Modeling of Liver Diseases

There are various cell culture and animal models that have been used to define mechanisms of liver development and pathogenesis. Conventional two-dimensional (2D) cell culture-based models have several limitations like insufficiency of long-term and stable cultures. In 2D primary hepatocyte culture, cells stop dividing and rapidly lose the liver-specific gene expression and function just a few weeks after plating (Bissell et al. 1987; Clayton and Darnell 2015; Mitaka and Ooe 2010). Moreover, they often lack cell-cell and cell-matrix interactions that are required to maintain *in situ* phenotypes and thus fail to mimic cellular functions and signaling pathways present in tissues (Baxter et al. 2015; Duval et al. 2017; Rowe and Daley 2019), which dramatically affects functions such as the synthesis of coagulation inhibitors (Boost et al. 2007), maintenance of stable cytochrome P450 expression (Darnell et al. 2012; Kostadinova et al. 2013) and integrin ligation (Meli et al. 2012). Furthermore, it is difficult to access fresh human liver sample to use for hepatocyte cultures but, ever since induced pluripotent stem cell (iPSC) technology was established, hepatocytes became producible in culture via stepwise differentiation protocols mimicking *in vivo* organogenesis (Chen et al., 2012; Hua, Yonghak, Saul, Luigi, & Yoon-Young, 2011; Si-Tayeb et al., 2010; Takahashi et al., 2007). Such step-wise protocols utilize cocktails of growth factors and cytokines to recapitulate embryonic liver development *in vitro*, from definitive endoderm to hepatic progenitors and then to functional hepatocytes.

2.2.1. Organoids for Disease Modelling

The definition of the organoid, as expressed by Hans Clevers, is: “a 3D structure grown from stem cells and consisting of organ-specific cell types that self-organizes.” (Clevers 2016). These structures, organoids, can be cultured long-term and stably maintain *in vivo* characteristics even after many generations, without any significant genetic or physiological changes (Huch et al. 2013). In the process of organoid culture, a number of growth factors and small molecules are used to control important signaling pathways in the self-renewal, differentiation, and proliferation often in a tissue-specific manner. For the last decade, organoids of different tissues (brain, kidney, liver, intestine pancreas, stomach and others) have been established and used for disease modelling (van den Berg et al. 2018; Huch et al. 2013, Huch et al. 2015; Lu et al. 2017; Watanabe et al. 2017; Wu et al. 2018). These organoid models use 3 different types of starting material, embryonic stem cells (ESC), induced pluripotent stem cells (iPSC) or adult stem cells (aSC). Since both ESC and iPSC are pluripotent stem cells (PSC), one can categorize organoids into 2 groups by their cell origin: PSC derived and aSC derived organoids (Clevers 2016). In Figure 2, established organoid models and their cell of origins are given.

2.2.1.1. Liver Organoids

One of the early works for the liver organoid establishment is the iPSC derived liver bud created by Taniguchi and his team, which iPSC cells were differentiated into hepatic endodermal cells and mixed with mesenchymal and endothelial cells for development of vascularization. After obtaining 3D mixed structures from these cells, the team of Taniguchi showed their vascularization is incorporated into the host’s system upon transplantation. Ultimately, these 3D structures showed hepatic functions in the host (Takebe et al. 2013). Another noteworthy model has established from aSCs in the same year by Huch and co-workers in which mouse Lgr5+ and human EpCAM+ progenitor cells were used to create hepatic organoids and these organoids maturation ability by either transplantation into the host or *in vitro* (Huch et al. 2013, Huch et al. 2015). Following these initial studies, many similar approaches have been established. Of those, Guan and colleagues also established hepatic organoids from iPSCs which consisted of both cholangiocytes that surround the lumina of ductal structures and hepatocytes. These organoids also had the regenerative capacity, resembling the human liver

(Guan et al. 2017). Our team has also been working on an iPSC derived hepatic organoid model for the modeling of Citrullinemia Type 1, and similarly, we have shown the long-term (>16 months) expansion and in vitro maturation capacity of these organoids which makes them amenable choices for disease modeling.

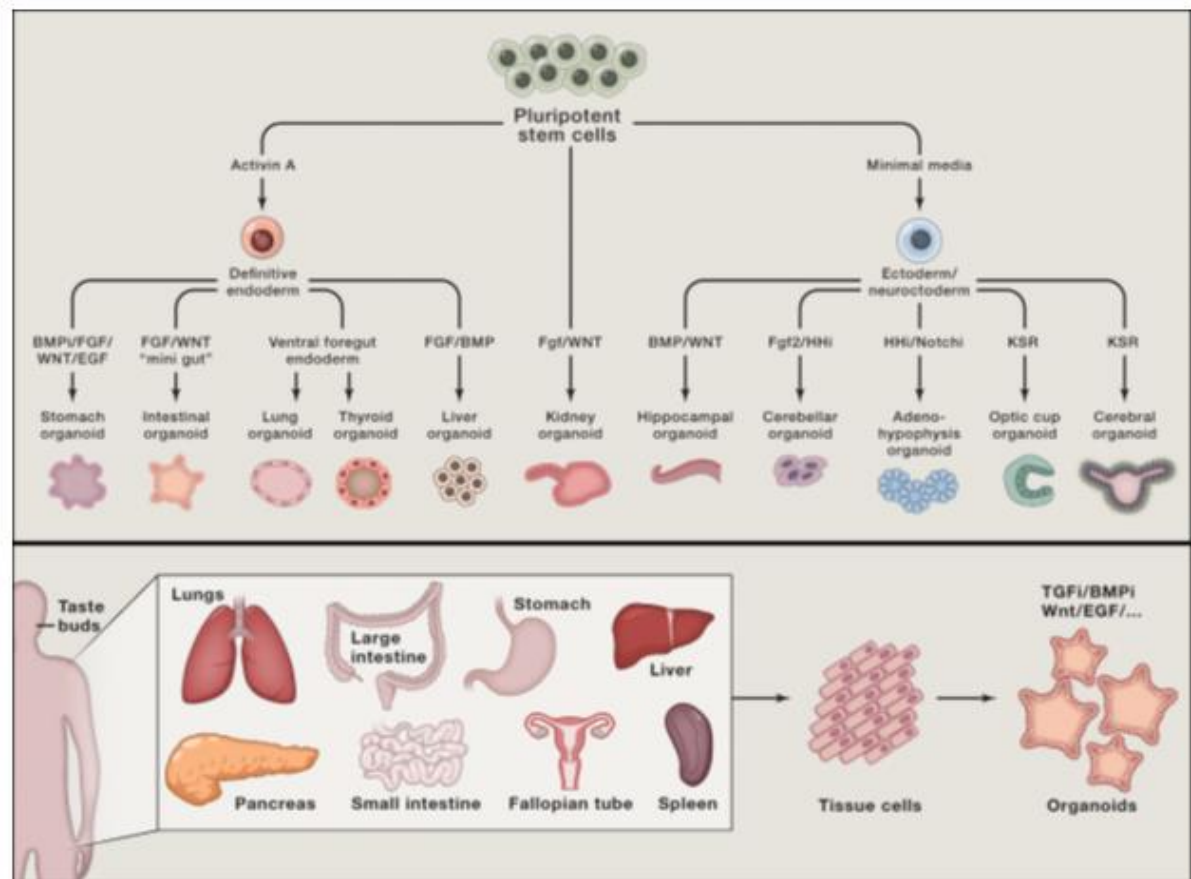


Figure 2: Established Organoid Models and Their Cell of Origins.

Pluripotent stem cell derived organoid models of endoderm and ectoderm origins (Top), Adult stem cell derived organoids of various organs (Bottom).

2.3. Wolman and Cholesterol Ester Storage Diseases

Wolman disease (WD) and cholesterol ester storage disease are cholesterol metabolism diseases caused by autosomal recessive mutations in the LIPA gene. WD has an incidence of 1 in 500,000 births and was regarded as a rare, orphaned disease. In contrast, CESD presents itself with a prevalence between 1 in 40,000 and 1 in 400,000. However, emerging evidence suggests

that this milder form is more common, yet undiagnosed (Carter et al. 2019; Hong Du et al. 2001; Frampton 2016).

The LIPA gene is found on chromosome 10 for humans and consists of 10 exons. RefSeq database declares 3 variants for the transcripts of this gene. First two isoforms encode for 399 amino-acid (AA) long proteins and the last one is a shorter one with 283 AAs. Human liver lysates for LAL purification has shown the presence of 56 and 41 kDa sized forms of LAL. Further analysis has shown that the 41 kDa version is enzymatically active form. Mannose 6-phosphate (M6P) aids in the trafficking of the protein in the cell and its delivery into the lysosome (Li & Zhang, 2019). Mutations of this gene results in either Wolman Disease (WD) or Cholesterol Ester Storage Disease (CESD). The most common mutation is a splice-junction mutation found on the exon 8 (E8SJM1G>A), and the findings suggest that E8SJM1G>A homozygote patients usually had an early-onset, slowly progressive disease (Bernstein et al. 2013). LAL is the enzyme encoded from LIPA gene and loss of function mutations of LIPA results in <1% LAL activity for WD and 1-5% LAL activity for CESD. Although CESD patients can survive through adulthood without being diagnosed, the life span of WD patients is under a year without treatment (Reiner et al. 2014). Both WD and CESD patients have fatty liver and splenomegaly as well as elevated LDL and lower HDL levels (Dubland & Francis, 2015). Similarly, the mouse model of LAL deficiency developed hepatosplenomegaly and showed accumulation of triglycerides and CEs in several organs including the liver and small intestine. Evaluation of the given model clarifies that complete deletion of *lal* in mice does not manifest itself as WD but rather as CESD (Du, Duanmu, Witte, & Grabowski, 1998). Therefore, mouse models of LAL deficiency have become a good model for human CESD and have since been used for many studies for the role of LAL in specific tissues or in the whole organism (H. Du 2001; Hong Du et al. 2005; Sun et al. 2014).

2.3.1. *The Role of LAL Enzyme in Health and Disease*

In a healthy hepatocyte, the role of LAL is the hydrolysis of low-density lipoproteins (LDLs): namely, cholesterol esters (CEs) and triglycerides into free cholesterol (FC) and free fatty acids (FFAs). Through this role, LAL takes a role in the lipid metabolism of several cell types such as hepatocytes and macrophages. The products of this reaction, FC and FFA modulate the cholesterol and lipid metabolism via SREBPs or LXR. *De novo* synthesis of FC, TG, CE are

regulated this way. Thus, the levels of cellular cholesterol and dependently, the levels of serum cholesterol are directly related to the LAL activity (Dubland and Francis 2015; Liangyou 2014; Reiner et al. 2014). Although it is such an important enzyme for the healthy lipid and, specifically cholesterol metabolism, there are limited studies on regulation and function of LAL. Therefore, there is a certain need for understanding the molecular pathways that have a role in these (Li and Zhang 2019; Wang et al. 2017).

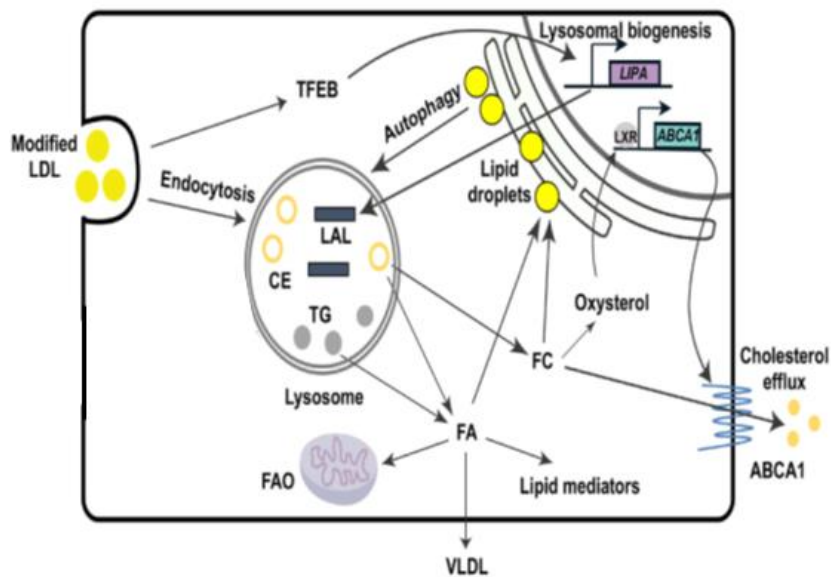


Figure 3: LAL enzyme working mechanism

LAL breaks down cholesteryl esters (CE) and triglycerides (TG) in the lysosome to fatty acids (FAs) and free cholesterol (FC). Released FC triggers the activation of LXR through oxysterol binding and increases the ABCA1 expression to remove the FC from cells.

Up to now, several studies have shown the regulators of the autophagy pathway, such as TFEB transcription factor (TF), also target the expression of the LIPA gene. Additionally, FOXO1, another TF involved in the autophagy pathway, has been shown to upregulate LIPA expression in adipocytes after nutrient restriction. Furthermore, LXR and PPAR agonists are known to increase the expression of LIPA via a non-explained mechanism since LIPA does not contain any known LXR or PPAR response region in its promoter. But free cholesterol (FC) in the cell can regulate the LXR activity towards reverse cholesterol metabolism. One of the genes of this process is ATP-binding cassette transporter A1 (ABCA1), which has been shown to be reduced in both CESD and Niemann Pick Disease type C (NPC) patients (H. Du 2001; Dubland and Francis 2015; Radović et al. 2016).

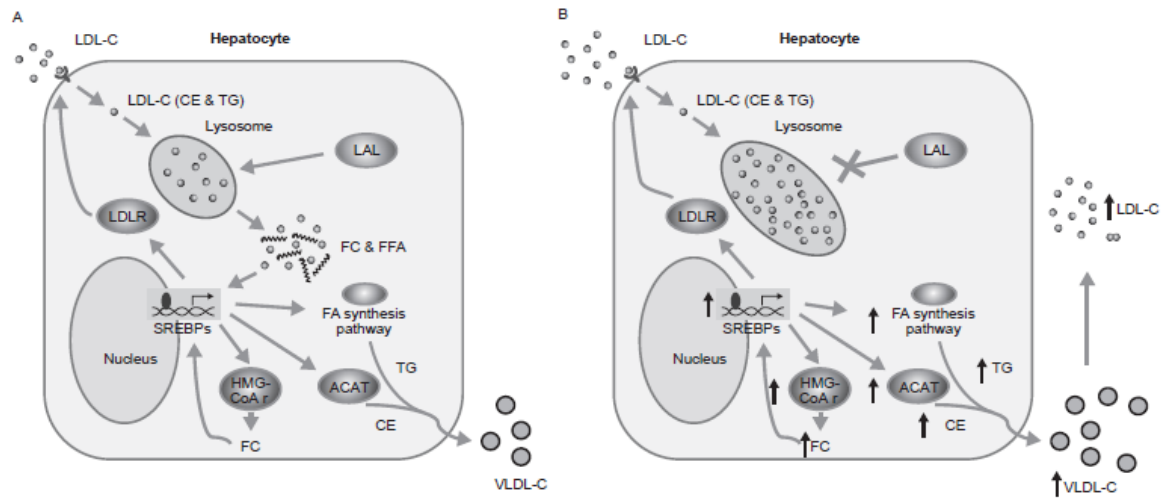


Figure 4: Cholesterol metabolism in healthy and LAL deficient hepatocytes

A. Healthy hepatocytes break down the TG and CE through LAL in lysosomes and released FFAs and FC regulate the lipid and cholesterol metabolism in the cell. B. LAL deficient hepatocytes cannot release FFAs and FC and thus the CE content of cell increases, to obtain FFAs the cell increases FA synthesis and similarly other pathways related to lipid and cholesterol metabolism.

In the case of LAL deficiency, the LDL particles taken into the cell start to accumulate in the lysosomes of the cells. In fact, in a mouse model of LAL deficiency, Radovic and co-workers have shown the lipid storage of *Lal*^{-/-} mice were within lysosomes as opposed to lipid droplets seen in WT mice. Since LDL is not hydrolyzed, the feedback mechanism to regulate *de novo* synthesis of FC, TG, CE is impaired, leading to increased synthesis of these molecules. As a result, the cell secretes excessive amounts of VLDL-C which is consistent with CE and TG to the bloodstream. In a mouse model of LALD, LDL-R expression was found to be unchanged even though the cellular LDL content was dramatically increased, suggesting that LDL uptake was not affected by LAL deficiency. Moreover, *de novo* cholesterol synthesis was shown to be increased in these mice, as expected. Similar to that of human, *Lal* deficient mice had increased LDL and decreased HDL levels while total cholesterol was increased in these mice (Dubland and Francis 2015; Radović et al. 2016).

2.3.2. Established Models of LALD and Treatment Strategies

The most commonly used models of LALD are animal models. The first animal model of LALD comes from a Japanese laboratory where a Donryu strain rat had spontaneously shown homozygous mutations in the Lipa gene and the characteristic human WD phenotype was observed. Later the parental rats with heterozygous Lipa mutation were identified and this LAL deficient rat strain was characterized and it is still maintained for the rodent studies of LALD (Kuriwaki and Yoshida 1999; Kuriyama Masaru et al., 1990). Another animal model of LALD is generated by Du et al. in 1998 with mice. These mice have the genotype of WD and represent WD pathology. But their lifespan represents CESD phenotype (Hong Du et al. 1998). The model has a healthy look at birth but develops hepatosplenomegaly between 4-8 weeks. Accumulation of CE and TG in hepatocytes and macrophages are also observed in these mice. Since then disease mechanism and treatment options are studied on these models. Earlier enzyme replacement therapy (ERT) approaches used recombinant human LAL (rhLAL) enzymes isolated from plant (Hong Du et al. 2008), yeast (H. Du 2001; Hong Du et al. 2005), CHO cells (Hong Du et al. 2005), human fibrosarcoma cell line (Sun et al. 2014), or expressed from viral vector system (Hong Du et al. 2002). All these studies showed the potential of the ERTs to control the disease progression and even reverse some of the complications. Both short term and long term trials of ERT was shown to extend the life span of the animals with the prevention of progressive lipid accumulation in the liver, spleen, and intestines of the animals. Of note, long term ERT was shown to reverse the disease phenotype evident from reduced lipid accumulation and reversal of the liver and spleen size to normal as well as a moderate recovery of liver fibrosis (Sun et al. 2014).

Apart from animal models, there are a limited number of *in vitro* LALD models/cell lines. Particularly, in a recent study, Aguisanda and co-workers have successfully generated patient-derived iPSCs to model Wolman Disease. As a proof of concept, the team has differentiated these iPSCs to neural stem cells and showed that LAL enzyme activity has been reduced in these patient-derived cells. Treatment of these cells with rhLAL has recovered activity loss of LAL enzyme (Aguisanda et al. 2017). Most importantly, Takebe and colleagues have also utilized the patient-derived iPSCs for a LALD model of the organoid. In the study, iPSC derived hepatic organoids with multiple cell types (hepatocyte, stellate, Kupffer and biliary cells) are

established, characterized and a steatohepatitis model is developed with healthy and WD organoids. In order to highlight the potential of the WD organoid model, the team also investigated the effects of a potential therapeutic agent, FGF-19 and found out that FGF-19 treatment has reduced the lipid accumulation and increased the survival of WD organoids. Thus, the team has pointed out new treatment options can be investigated with their *in vitro* model (Ouchi et al. 2019).

Sebalipase alfa, the only FDA approved curative treatment option for LALD is also a recombinant human LAL (rhLAL) enzyme replacement. It is produced from transgenic hens' egg whites. The recombinant enzyme has the same AA sequence as humans and it also has the same post-transcriptional modifications such as M6P modification. Previous studies of rhLAL had different/inadequate mannose modifications which had changed the cellular uptake dynamics of the enzyme (Hong Du et al. 2005). During drug development of the Sebalipase alfa, the cellular uptake of the rhLAL into macrophages and fibroblasts have been shown. Following drug administration, the rescue of LAL enzyme activity was also shown in the patient fibroblasts (Frampton 2016). Later, for the preclinical phase, animal (rat) model of the disease has been used to show the efficacy of the drug to correct liver lipid levels and serum transaminase levels to show a reduction in liver damage (Thelwall et al. 2013).

3. MATERIALS AND METHOD

3.1 Type of Study

It is an experimental study.

3.2 Time and Location of Study

The research was conducted at Izmir Biomedicine and Genome Center, between January 2019 and May 2019.

3.3 Population and Sample of Study

Our study was performed with iPSCs obtained from healthy volunteers and cell lines HepG2, Huh-7.

3.4 Materials of Study

Induced pluripotent stem cells (iPSC), which we obtained from our Tubitak 1003 project (#213S182), was used as starting material for obtaining both two-dimensional hepatocytes and organoid model. Also, HCC cell line Huh7 was used as control samples or for optimization experiments.

3.5 Variables of the Study

Hepatic progenitor cells derived from iPSCs, hepatocytes differentiated from these iPSCs, their organoid cultures and other cell lines Huh7 are independent variables. LIPA expression level of different cell lines and cultures, change of LAL enzyme activity under different culture conditions are dependent variables.

3.6. Tools for Data Collection

3.6.1. Starting Material

In a previously completed Tubitak 1003 project, which was conducted jointly by Koç University and Dokuz Eylül Universities, we already produced induced pluripotent stem cells (iPSC) from primary fibroblast cells taken from healthy volunteers and these iPSCs were used as starting material to create an organoid model as well as for differentiation of 2D hepatocytes.

3.6.2. Conditional Knock-Down of LIPA Gene in iPSCs

3.6.2.1 shLIPA and Non-Target Control Plasmid Preparation

For plasmid preparation, glycerol stocks of shRNA for LIPA gene (V3SH11252-227076669 (sh1), V3SH11252-228936549 (sh2), V3SH11252-230034129 (sh3)) and non-target control (VSC11653 (NTC)) were streaked with the tip of sterile 10 µl pipette tip and were used to inoculate 5 ml of LB broth medium with 100 µg/mL ampicillin. Bacteria were incubated at 37°C at 180 rpm for 8 hours.

Table 2-1: shRNA sequences and product numbers

	Dharmacon Product #	Sequence	Target
ShRNA-1	V3SH11252- 227076669	TGTGGGAGGATAACTCTGG	targets ORF
ShRNA-2	V3SH11252- 228936549	AACTGAGAGTGTCTTATGT	targets ORF
ShRNA-3	V3SH11252- 230034129	TTACAAAGTAGTATTCGCC	targets 3'UTR

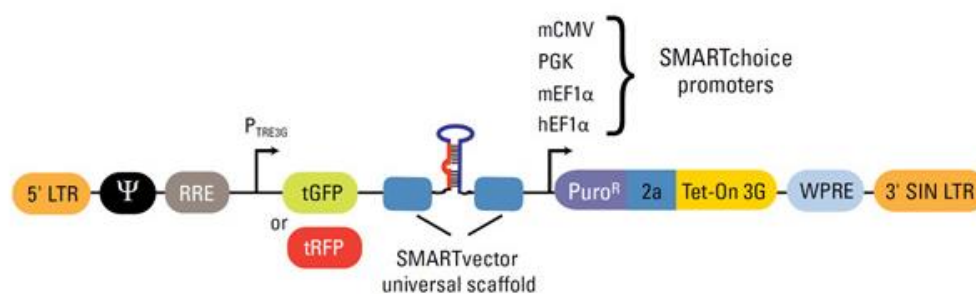


Figure 5: The map of inducible lentiviral shRNA construct

Under hEF1 α promoter Puromycin resistance and Tet-On-3G proteins are expressed constitutively and doxycycline inducible TRE3G promoter expresses tGFP/tRFP protein as well as the shRNA of interest.

3.6.2.2 Plasmid DNA Midiprep

Qiagen Plasmid Plus Midi Kit was used according to manufacturer's protocol to obtain vector DNA and their concentration was measured using nanodrop.

3.6.2.3 Production of Lentiviral shRNA Constructs in Hek293T Cell Line

To obtain the lentiviral particles of the sh1, sh2, and sh3 vectors, which provide silencing of LAL gene, and a non-target control (NTC) to check our system, 5.5×10^6 Hek293T cells were plated into 10-cm plates and incubated overnight at 37°C with 5% CO₂. Next day, Trans-Lentiviral Packaging Kit was mixed with vector DNA for each construct and Hek293T cells were transfected. After 10-16 hours, the transfection medium was replaced with reduced serum (5% FBS) medium and cells were incubated for an additional 48 hours. Then, the supernatant was collected and centrifuged at 1200×rpm at 4°C for 5 minutes to pellet cell debris and the supernatant was purified from any remaining cell debris using a 0.45 μ M filter. Viral particles were either used fresh or stored in -20°C for up to 4 weeks.

3.6.2.4 Establishing LAL Deficient Stable iPSC Lines

iPSCs were plated in Matrigel-coated 12 well plates and colonies were grown to an appropriate size, then 1 mL of the viral particle was replaced with culture medium with 1 μ L of 8mg/mL polybrene. Next day, the transduction culture medium was replaced with mTESR medium. One

day later, 1 µg/mL puromycin was added to mTESR growth medium to select the cells with the viral construct. After a week, puromycin was withdrawn from the culture medium. 1 mg/mL doxycycline was used to induce shRNA expression on these cells. 3 days after induction with doxycycline, cell pellets were collected for RNA isolation. Following cDNA synthesis, gene knock-down was checked via qPCR.

3.6.3. Generation of iPSC Derived Mature Hepatocytes

iPSCs were cultured with mTESR1 medium in Matrigel-coated plates. After the cell density reached 70%, the culture medium was replaced with RPMI medium supplemented with 1X B27, containing 100 ng/mL activin A, 50 ng/mL Wnt3a, and 10 ng/mL HGF for 3 days, after this period cells were differentiated into endoderm cells. Then, to obtain hepatic progenitor cells medium was replaced with DMEM supplemented with 20% knock-out serum replacement, containing 1 mM L-glutamine, 1% non-essential amino acids, 0.1 mM 2-mercaptoethanol and 1% dimethyl sulfoxide for 4 days. For the final stage, progenitor cells were cultured in IMDM medium containing 20 ng/mL oncostatin M, 0.5 µM dexamethasone and 50 mg/mL ITS premix for 4 days to differentiate into mature hepatocytes. (Chen et al., 2012a).

3.6.4. Generation of Endodermal Hepatic Organoids (eHEPOs)

The protocol for the eHEPO generation consists of 2 steps: (1) 2D differentiation of iPSCs to DE and (2) 3D structure formation from EpCAM⁺ DE cells. The detailed protocols are explained below.

3.6.4.1. Differentiation of iPSCs to Endoderm and Hepatic Progenitor Cells

iPSCs were cultured with mTESR1 medium in Matrigel-coated plates. After the cell density reached 70%, the culture medium was replaced with RPMI medium supplemented with 1X B27, containing 100 ng/mL activin A for 5 days, after this period cells were differentiated into endoderm cells (Si-Tayeb et al. 2010).

3.6.4.2. Separation of EpCAM + Cells by FACS

Cell suspensions of the induced endoderm from iPSCs are sorted for their EpCAM expression. First, cells were counted with trypan blue to determine the number of viable cells. 10^6 cells/ml in FACS buffer was passed through 100 μ m and 40 μ m mesh. After centrifugation, the pellet was dissolved with 100 μ l FACS buffer for 10^7 cells and incubated with 1:50 anti-CD326 (EpCAM)-FITC antibody for 10 min at 4°C at dark. After washing, the pellet was dissolved in FACS buffer and EpCAM+ cells were separated by flow cytometry.

3.6.4.3. Formation and Expansion of eHEPO Culture

The separated cells were centrifuged and the resulting cell pellet was cultured according to the protocol below, published by Huch et al. (2015a). Cells were mixed with matrigel with a ratio of matrigel to cell suspension of 7:3 and seeded in 24-well (non-adherent) cell culture plates to contain 5000 cells/well. These cells were cultured in Expansion Medium (EM) which consisted of Advanced DMEM /F12 with 1% B27 without vitamin A and 1.25mM N-acetylcysteine, 10nM gastrin, 50ng/ml EGF, 10% RSPO1 conditioned medium(CM) (home-made), 100ng/ml FGF-10, 25ng/ml HGF, 10mM Nicotinamide, 5uM A83.01, 10uM Forskolin. For the first 3 days after culture establishment, EM is supplemented with 25 ng/ml Noggin, 30% Wnt CM (home-made) and 10uM Y27632. After 10-14 days, the organoids were removed from the matrigel, mechanically dissected and transferred into the fresh matrix. When matrigel was solidified, EM culture medium was added. The passage was performed at a rate of 1:2 to 1:4 every 7-10 days.

3.6.4.4. Differentiation to Functional eHEPOs

Organoids have grown to have a diameter of minimum 100 μ m in EM, then the culture medium was changed to Differentiation Medium (DM) and the medium was replenished every 2-3 days for 10-14 days. Differentiation Medium is consisted of Advanced DMEM /F12 with 1% B27 without vitamin A and 10nM gastrin, 50ng/ml EGF, 100ng/ml FGF-19, 25ng/ml HGF, 500nM A83.01, 10uM DAPT, 25ng/ml BMP-7, 30uM Dexamethasone.

3.6.5. Characterization of eHEPOs

3.6.5.1. Gene Expression Analysis

RNA isolation

Cell culture plates cultured with 2D hepatocytes were washed with 1x PBS and cell pellets were collected using 500 μ L TRIZOL. For eHEPO samples, the medium has aspired and 500 μ L TRIZOL was directly added onto the Matrigel drops and the mixture was run through an insulin syringe to ensure the breaking-down of Matrigel for complete lysis of the cells. After this step, 100 μ L chloroform was added to both kind of samples and incubated for 5 minutes at room temperature. Followed by a 15-minute 12,000 rpm centrifugation step, the upper phase of the solution was collected into a new tube and 70% ethanol was added. This mixture was then loaded onto the columns of the GeneJET RNA purification kit and manufacturer's protocol was followed after this step. The resulting RNA pellet was dissolved in 30 μ L DNase/RNase free water and concentration of RNA was measured using nanodrop.

cDNA Synthesis

Maxima First Strand cDNA synthesis kit for RT-qPCR was used according to the manufacturer's protocol. Briefly, the following components were pipetted into a PCR tube and the reaction was run at 25°C for 10 minutes followed by a 50°C for 30 minutes and finally 85°C for 5 minutes. Obtained cDNA was diluted to obtain a concentration of 5 ng/ μ l and stored at -20°C for future use.

Table 2-2: cDNA synthesis reaction set up

5X Reaction Mix	4 μ L
Maxima Enzyme Mix	2 μ L
Template RNA	500ng - 1 μ g
Water, nuclease-free	to 20 μ L
Total volume	20 μ L

Quantitative Real-Time PCR

For the qPCR reactions either Power SYBR Green PCR master mix or TaqMan Universal master mix II with no UNG was used with the following recipes:

Table 2-3: Quantitative real-time PCR reaction set up with SYBR Green reagent

Power SYBR Green PCR master mix	5 μ L
F and R primers	1 μ L
Water, nuclease-free	3 μ L
cDNA (5ng/ μ L)	1 μ L
Total volume	10 μ L

The reactions were set as 95°C for 15 minutes for 1 cycle, 95°C for 15 seconds, 60°C for 1 minute for 40 cycles for the TaqMan reagent and 95°C for 10 minutes for 1 cycle, 95°C for 10 seconds, X°C for 20 seconds and 72°C for 40 seconds for 40 cycles, where X is the T_m for that primer set for the SYBR Green reagent.

Table 2-4: Primer Sequences and T_m values

Gene	Sequence	T _m
RPL41-F	GGCCTTAGCGCCATTTTT	60
RPL41-R	TTGGACCTCTGCCTCATCTT	60
LIPA-F	CTGTAAATTCCAAAAGTTTCAAGC	60
LIPA-R	CTGGTTGTAATGAAAATAATTCTTGG	60

3.6.5.2. Functional Analysis

To assess the functionality of the mature eHEPOs Albumin secretion was measured via ELISA assay and lipid storage capacity was shown with immunofluorescent lipid (IF) LD staining.

3.6.5.2.1. ELISA Assay for Albumin Secretion

Cell culture supernatants of both 2D and 3D hepatocyte cultures were collected and stored at -20°C until the assay was performed. Bethyl Biotechnologies Human Albumin ELISA kit was used according to the manufacturer's protocol for the detection of albumin in the cell culture medium. Briefly, the wells were coated with diluted anti-human albumin antibody 16 hours prior to the experiment. The next day, wells were washed and blocked for 1 hour, followed by a 1-hour incubation step with the cell culture supernatant. Then the wells were incubated with

diluted HRP-conjugated anti-human antibody for another hour and then after another washing step, TMB substrate was added onto each well. After 15-minute-long incubation at room temperature, protected from light, the reaction was stopped. The color intensity of each well was measured using Varioskan Flash and a standard curve was interpolated to determine the concentration per sample. Obtained results were normalized for cell number.

3.6.5.2.2. Monodansylpentane (MDH) Staining

For 2D samples the cells were fixed with 4% PFA for 20 minutes, followed by PBS wash. Then the samples were incubated with MDH diluted in 0.1% BSA containing PBS (PBS-B) (1:1000) for 30 minutes. Then the samples were washed twice with PBS and the nuclei were stained with PI (1:100) in PBS for 30 seconds followed by PBS wash.

For 3D samples, the organoids were collected from wells with ice-cold PBS-B and transferred to falcons. The volume of the PBS-B in the falcons was completed to 10 mL. After 10-minute incubation on ice, the supernatant was carefully removed without disturbing the organoids in the bottom of the tube. Fresh, ice-cold PBS-B was added to the tube and the same procedure was repeated for a total of 3 times. Afterwards, all of the PBS-B was removed, taking care not to remove the organoids, to fix the organoids 4% PFA was added and organoids were incubated for 30 minutes on ice. Afterwards, the above-explained washing procedure was repeated for 3 times and subsequently, the staining with MDH in PBS-B (1:1000) was performed for 1 hour at RT. Then the samples were washed with PBS three times and the nuclei were stained with PI (1:100) in PBS for 1 minute followed by PBS wash.

3.6.6. LAL Enzyme Activity Determination

For the LAL enzyme activity determination 2D cells were scraped from the wells and washed with PBS, eHEPO samples were collected using ice-cold PBS-B and to remove matrigel 10-minute ice-cold PBS wash was performed 3 times, then the organoids were pipetted through glass Pasteur pipettes with narrowed tips to remove any remaining matrigel. Both 2D and 3D samples were kept on ice during this preparation process.

3.6.6.1. Homogenization of Samples

Ultra sonication was performed for the homogenization of the samples. 500 µl 0.1 M sodium acetate buffer was used per sample for 5 minutes. During homogenization, the samples were kept on ice and the sonication was performed with a 15 secs on-30 secs off-cycle for 5 minutes. Then the samples were centrifuged at 17,000g for 1 hour and the upper phase was collected for determination of LAL enzyme activity and protein concentration.

3.6.6.2. Enzyme Activity Assay

Samples from the previous step were distributed to 96 well-plates with black walls. For the inhibited reactions, 4-methylumbelliferyl palmitate as substrate, cardiolipin as activator and Lalstat as inhibitor was added to selected wells. For the uninhibited reactions, everything else except inhibitor was added to the wells. Instead of inhibitor, the same volume of water was added to obtain equal reaction volume. The plate was incubated at 37°C for 24 hours, protected from light. To stop the reaction 150 mM EDTA was added to the wells then fluorometric measurement was taken using Varioskan Flash (ex/em 320/450 nm).

3.6.6.3. Determination of Protein Concentration

Pierce BCA protein assay kit was used according to the manufacturer's protocol for the determination of protein concentration. Briefly, 25 µl of sample or control was added to each well of 96-well plate and 200 µl working reagent was added to each well. After a 30-minute incubation at 37°C absorbance was read at 562nm. Sample concentrations were calculated from the standard curve and the enzyme activity was normalized using these values.

3.6.7. Materials Used

Materials used in this thesis are given in the table below with their catalog numbers and vendors.

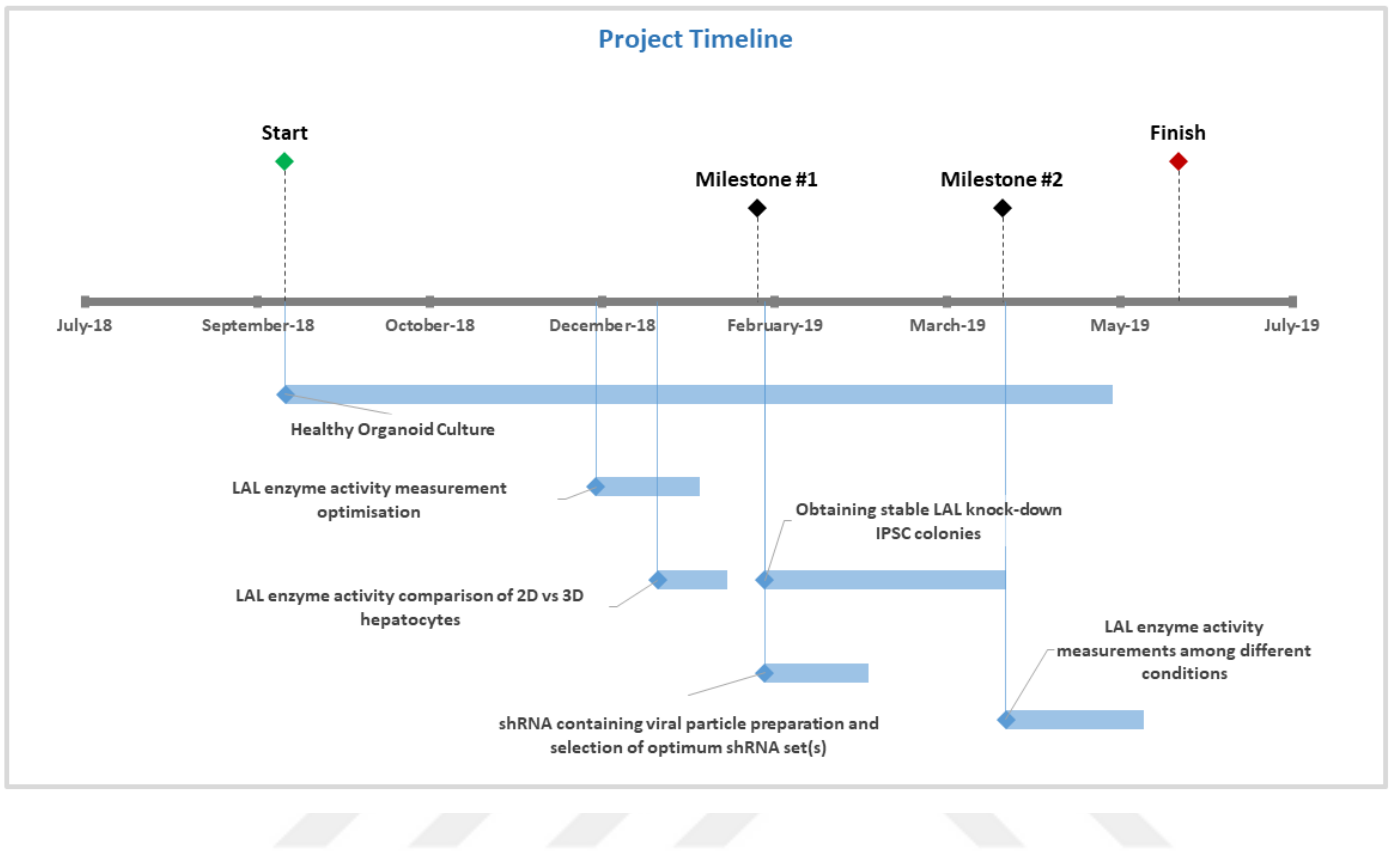
Table 2-5: Materials with catalog numbers

Material	Catalog #	Vendor
mTeSR 1 Basal Medium	85851	StemCell Technologies
mTeSR1 5x Supplement	85852	StemCell Technologies
ReLESR	05872	StemCell Technologies
Matrigel-hESC qualified matrix	354277	Corning
Matrigel	356231	Corning
mFreSR	05855	StemCell Technologies
DMEM	41965-039	Gibco
DMEM/F12	31330-038	Gibco
Advanced DMEM/F12	12634-010	Gibco
Qiagen Plasmid Plus Midi Kit	12943	Qiagen
Thermo GeneJET RNA purification Kit	K0731	Thermo Scientific
Maxima First Strand cDNA synthesis kit for RT-qPCR	K1642	Thermo Scientific
Trans-Lentiviral Packaging Kit	TLP5914	Dharmacon

Table 2-6: Equipment list

Device	Brand
Nanodrop 2000	Thermo Scientific
Centrifuge MicroCL 17R	Thermo Scientific
Centrifuge 5810R	Eppendorf
Applied Biosystems 7500/7500 Fast	Applied Biosystems
VarioSkan Flash	Thermo Scientific

3.7. Study Plan and Calendar



3.8. Data Evaluation

GraphPad Prism 7.1, Flow Jo V10, ImageJ 1.52a programs were used to analyze/present the findings. Student's t-test and ANOVA were used for statistical analysis, significance values were taken as *P < 0.05, **P < 0.001, and ***P < 0.0001. Flow Cytometry analyses were performed using Flow Jo V10 and Image enhancements were performed using ImageJ 1.52a.

3.9. Limitations of the Study

The goal of this study was to develop a 3D in vitro model for Cholesterol Ester Storage Disease (CESD). The main limitation of the study is the lack of monoclonal LAL silenced colonies; our experimental design did not include a time period for such a lengthy process. This can be improved by selecting GFP positive single cells and growing colonies from these cells. Also, this thesis used a limited number of shRNAs and thus, obtained a limited degree of gene

silencing. Rescue experiments using LAL enzyme replacement or LAL overexpression vectors could be included for better justification of the model.



3.10. Ethics Committee Approval

DOKUZ EYLÜL ÜNİVERSİTESİ
GİRİŞİMSEL OLMAYAN ARAŞTIRMALAR ETİK KURUL KARARI

Sayın Prof.Dr. Nur Arslan

Araştırmanıza ilişkin Kurulumuz kararı aşağıda sunulmuştur.

Bilgilerinizi ve gereğini rica ederiz.

ETİK KOMİSYONUN ADI	DOKUZ EYLÜL ÜNİVERSİTESİ GİRİŞİMSEL OLMAYAN ARAŞTIRMALAR ETİK KURULU
AÇIK ADRES	Dokuz Eylül Üniversitesi Tıp Fakültesi Dekanlığı 2. Kat İnciraltı-İZMİR
TELEFON	0 232 412 22 54-0 232 412 22 58
FAKS	0 232 412 22 43
E-POSTA	etikkurul@deu.edu.tr

BAŞVURU BİLGİLERİ	DOSYA NO:	4685-GOA
	ARAŞTIRMA	UZMANLIK TEZİ <input type="checkbox"/> MÜNFERİT ARAŞTIRMA <input type="checkbox"/> ÖÇM <input type="checkbox"/> YÜKSEKLİSANS <input checked="" type="checkbox"/> DOKTORA <input type="checkbox"/>
	ARAŞTIRMANIN AÇIK ADI	3 Boyutlu Hepatik Organoidlerde Lizozomal Asit Lipaz Eksikliği Modelinin Geliştirilmesi
	ARAŞTIRMA PROTOKOL KODU	
	SORUMLU ARAŞTIRMACI ÜNVANI/ADI/SOYADI ve UZMANLIK ALANI	Prof.Dr. Nur Arslan Çocuk Sağlığı ve Hastalıkları A.D.
	ARAŞTIRMAYA KATILAN MERKEZLER	TEK MERKEZ <input checked="" type="checkbox"/> ÇOK MERKEZLİ <input type="checkbox"/>

DEĞERLENDİRİLEN BELGELER	Belge Adı	Tarihi	Versiyon Numarası	Dili		
	ARAŞTIRMA PROTOKOLÜ	Mevcut		Türkçe <input checked="" type="checkbox"/>	İngilizce <input type="checkbox"/>	Diğer <input type="checkbox"/>
	ARAŞTIRMA İLE İLGİLİ LİTERATÜR	Mevcut		Türkçe <input type="checkbox"/>	İngilizce <input checked="" type="checkbox"/>	Diğer <input type="checkbox"/>
	BİLGİLENDİRİLMİŞ GÖNÜLLÜ OLUR FORMU	Mevcut		Türkçe <input checked="" type="checkbox"/>	İngilizce <input type="checkbox"/>	Diğer <input type="checkbox"/>
	OLGU RAPOR FORMU	Mevcut		Türkçe <input checked="" type="checkbox"/>	İngilizce <input type="checkbox"/>	Diğer <input type="checkbox"/>

KARAR BİLGİLERİ	Karar No:2019/08-27	Tarih:03.04.2019
	Prof.Dr. Nur Anılan'ın sorumlusu olduğu "3 Boyutlu Hepatik Organoidlerde Lizozomal Asit Lipaz Eksikliği Modelinin Geliştirilmesi" isimli klinik araştırmaya ait başvuru dosyası ve ilgili belgeler araştırmanın gerekece, amaç, yaklaşım ve yöntemleri dikkate alınarak incelenmiş, etik açıdan çalışmanın gerçekleştirilmesinin uygun olduğuna oy birliği ile karar verilmiştir.	
ETİK KURUL BİLGİLERİ		
ÇALIŞMA ESASI	Dokuz Eylül Üniversitesi Girişimsel Olmayan Araştırmalar Etik Kurulu İşleyiş Yönergesi İyi Klinik Uygulamalar Kılavuzu	
ETİK KURUL ÜYELERİ		

Unvanı/Adı/Soyadı	Uzmanlık Alanı	Kurumu	Cinsiyet	Araştırma ile İlgili mi?		İmza
Prof.Dr.Can SEVİNÇ (Başkan)	Göğüs Hastalıkları	DEÜ Tıp Fakültesi Göğüs Hastalıkları A.D	Erkek	E <input type="checkbox"/>	H <input checked="" type="checkbox"/>	
Prof.Dr.Sadık Kıvanç MİTEN (Başkan Yardımcısı)	Kalp ve Damar Cerrahisi	DEÜ Tıp Fakültesi Kalp Damar Cerrahisi Anabilim Dalı	Erkek	E <input type="checkbox"/>	H <input checked="" type="checkbox"/>	
Prof.Dr.Arzu GÜNEÇ	Nörolojik Fizyoterapi - Fizik Tedavi ve Rehabilitasyon	DEÜ Fizik Tedavi ve Rehabilitasyon Yüksek Okulu	Kadın	E <input type="checkbox"/>	H <input checked="" type="checkbox"/>	
Prof.Dr. Sema ÖZKAL	Tıbbi Patoloji	DEÜ Tıp Fakültesi Tıbbi Patoloji A.D	Kadın	E <input type="checkbox"/>	H <input checked="" type="checkbox"/>	
Prof.Dr.Fırat TUNCEL	Tıbbi Biyokimya	DEÜ Tıp Fakültesi Tıbbi Biyokimya Anabilim Dalı	Kadın	E <input type="checkbox"/>	H <input checked="" type="checkbox"/>	Katılmadı.
Prof.Dr.Serkan YENER	Endokrinoloji	DEÜ Tıp Fakültesi İç Hastalıkları Anabilim Dalı	Erkek	E <input type="checkbox"/>	H <input checked="" type="checkbox"/>	
Doç.Dr.Nil Hocaoğlu AKSAY	Tıbbi Farmakoloji	DEÜ Tıp Fakültesi Tıbbi Farmakoloji Anabilim Dalı	Kadın	E <input type="checkbox"/>	H <input checked="" type="checkbox"/>	
Doç.Dr.Murat BEKTAS	Çocuk Sağlığı ve Hastalıkları Hemşireliği	DEÜ Hemşirelik Fakültesi Çocuk Sağlığı ve Hastalıkları Hemşireliği	Erkek	E <input type="checkbox"/>	H <input checked="" type="checkbox"/>	
Doç.Dr.Telâh ÇANKAYA	Tıbbi Genetik	Tıbbi Genetik Anabilim Dalı	Erkek	E <input type="checkbox"/>	H <input checked="" type="checkbox"/>	
Doç.Dr. Ayfer DAYI	Davranış Fizyolojisi	DEÜ Tıp Fakültesi Fizyoloji Anabilim Dalı	Kadın	E <input type="checkbox"/>	H <input checked="" type="checkbox"/>	
Doç.Dr.Korcan DEMİR	Pediyatrik Endokrinoloji	DEÜ Tıp Fakültesi Çocuk Sağlığı ve Hastalıkları Anabilim Dalı	Erkek	E <input type="checkbox"/>	H <input checked="" type="checkbox"/>	
Doç.Dr.Mahmut Can ERGÖN	Tıbbi Mikrobiyoloji	DEÜ Tıp Fakültesi Tıbbi Mikrobiyoloji Anabilim Dalı	Erkek	E <input type="checkbox"/>	H <input checked="" type="checkbox"/>	
Öğr.Gör.Dr.Kıvanç YÜKSİL	Biyostatistik ve Tıbbi Bilgi	Ege Üniversitesi Tıp Fakültesi Biyostatistik ve Bilgi A.D	Erkek	E <input type="checkbox"/>	H <input checked="" type="checkbox"/>	
Av. Esra FIRTINA	Avukat	DEÜ Rektörlüğü Hukuk Müşavirliği	Kadın	E <input type="checkbox"/>	H <input checked="" type="checkbox"/>	
Mehmet Emin ÖZKUL	Sağlık mensubu olmayan üye	DEÜ Tıp Fakültesi İdari Mali İşler	Erkek	E <input type="checkbox"/>	H <input checked="" type="checkbox"/>	

4. RESULTS

4.1. Development of 2D and 3D Hepatocyte Cultures from iPSCs

In our previous work, we have generated iPSCs from a healthy donor via episomal reprogramming (Akbari S.). We then separately differentiate iPSCs to endoderm and produce functional 2D mature hepatocyte and 3D hepatic organoid named as eHEPO in this study. The schematic representation of the workflow with representative bright-field (BF) images was shown in Figure 6.

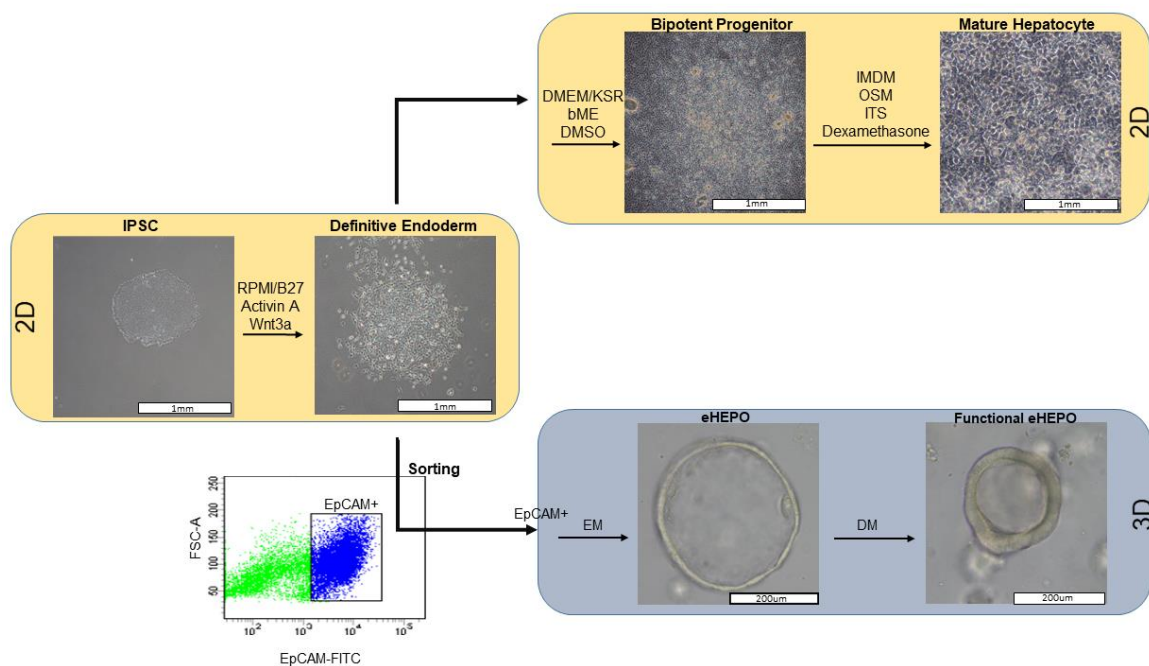


Figure 6: Schematic representation of work-flow and representative BF images.

BF images of iPSC, Definitive Endoderm (DE), Bipotent Progenitor (BP) or Mature Hepatocytes (MH) (Yellow panel), Representative BF images of endodermal hepatic organoid (eHEPO) and functional eHEPO (Dark blue panel).

4.1.1. Differentiation of iPSCs to Definitive Endoderm

Healthy iPSC colonies were induced with Activin A and Wnt3a for differentiation into the endodermal lineage, after 5 days of induction the cells were checked for the expression of stem cell and endodermal markers with flow cytometry and immune fluorescence (IF) staining. In flow cytometry analysis, expression of OCT-4 and Nanog for the iPSC cells were observed and

while the expression of FOXA2, demonstrating the differentiation into endodermal lineage has been shown in the definitive endoderm (DE) cells. Similarly, IF stainings showed the expression of endodermal markers, FOXA2, SOX17 and EpCAM in DE cells (Figure 7).

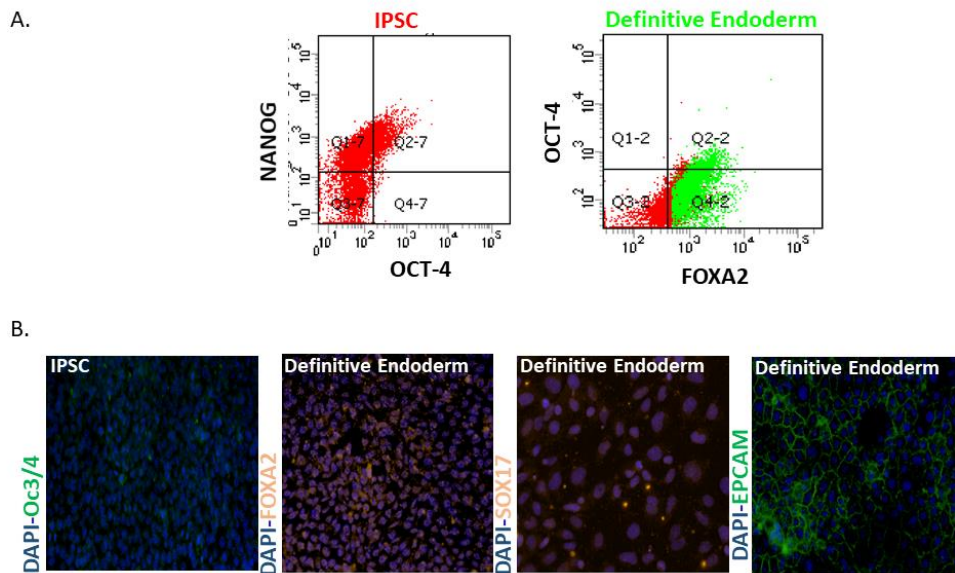


Figure 7: Flow Cytometry analysis and Immune Fluorescence (IF) stainings of iPSC colonies and DE cells.

A. Expression of NANOG/OCT-4 in iPSC cells and OCT-4/FOXA2 in DE cells as observed in flow cytometry.
 B. IF stainings of OCT3/4 in iPSCs, FOXA2,SOX17 and EpCAM in DE cells (Bottom).

4.1.2. Development of 2D Hepatocyte Culture from iPSCs

2D hepatocytes were obtained using the protocol by Chen and his colleagues. This 3 step differentiation protocol has been used by our team previously and the reproducibility of the protocol and characterization of these cells were previously done for another project. At the bipotent progenitor (BP) stage, these cells express AFP and HNF4a, shown via flow cytometry and IF stainings. Finally, at the mature hepatocyte (MH) stage, A1AT and albumin stainings were performed. To confirm their functionality, albumin secretion of the cells were measured (Figure 8).

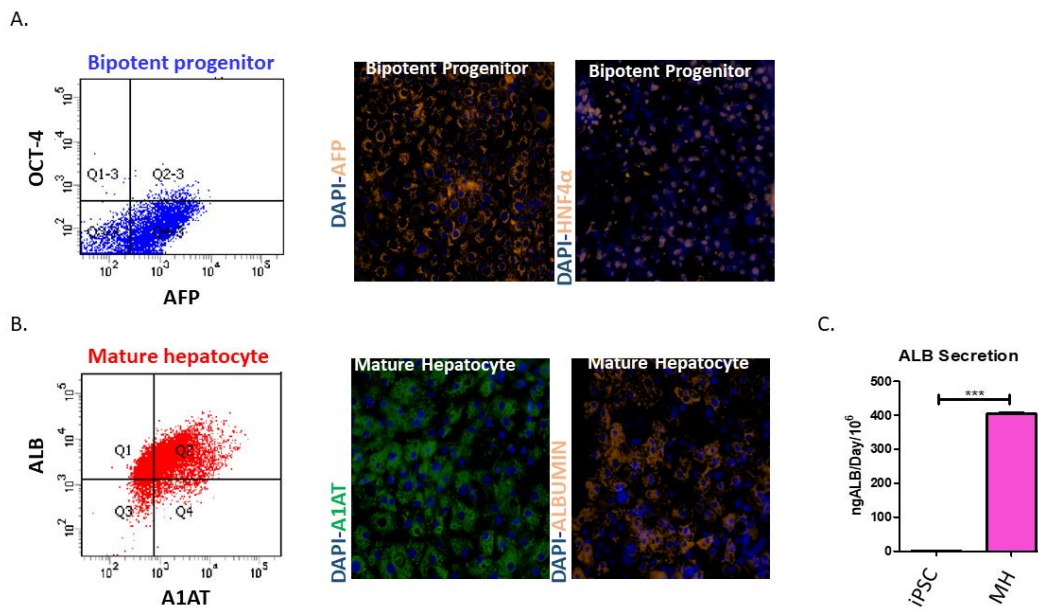


Figure 8: Flow Cytometry analysis and Immune Fluorescent (IF) stainings of BP and MH cells and Albumin ELISA assay for the hepatocyte function.

- A. OCT-4/AFP staining of bipotent progenitor cells as observed in flow cytometry. IF staining of AFP and HNF4a.
- B. ALB/A1AT staining of mature hepatocytes as observed in flow cytometry. IF staining of ALB and A1AT.
- C. Albumin secretion of mature hepatocytes as measured by ELISA.

4.1.3. Development of 3D Endodermal Hepatic Organoid (eHEPO) Culture from iPSCs

Healthy eHEPOs were previously produced and characterized by our team (Akbari S. et al., under revision). The same production method was also utilized. Briefly, the iPSC cells were differentiated to DE, then EpCAM⁺ cell population was sorted. The sorted cells were embedded in matrigel and cultured under defined culture conditions. The schematic representation of this workflow is given in Figure 6.

4.1.3.1. Hepatic Organoids in Expansion Phase (EM) and After Maturation Phase (DM)

After approximately 7-10 days in EM culture conditions, the organoids were formed and they were expanded as much as needed with 1:2 – 1:4 ratio until the desired number of organoids were obtained. We have previously shown that these organoids can be expanded up to 48 passages (approximately 16 months) and they still show functionality when differentiated in

DM conditions. To show their functionality a series of assays were performed such as Albumin ELISA, CYP3A4 activity assay, glycogen storage and LDL-uptake stainings which are presented in our recent work (Akbari S., 2019). Of these, Albumin secretion and LDL-uptake are shown in Figure 9.

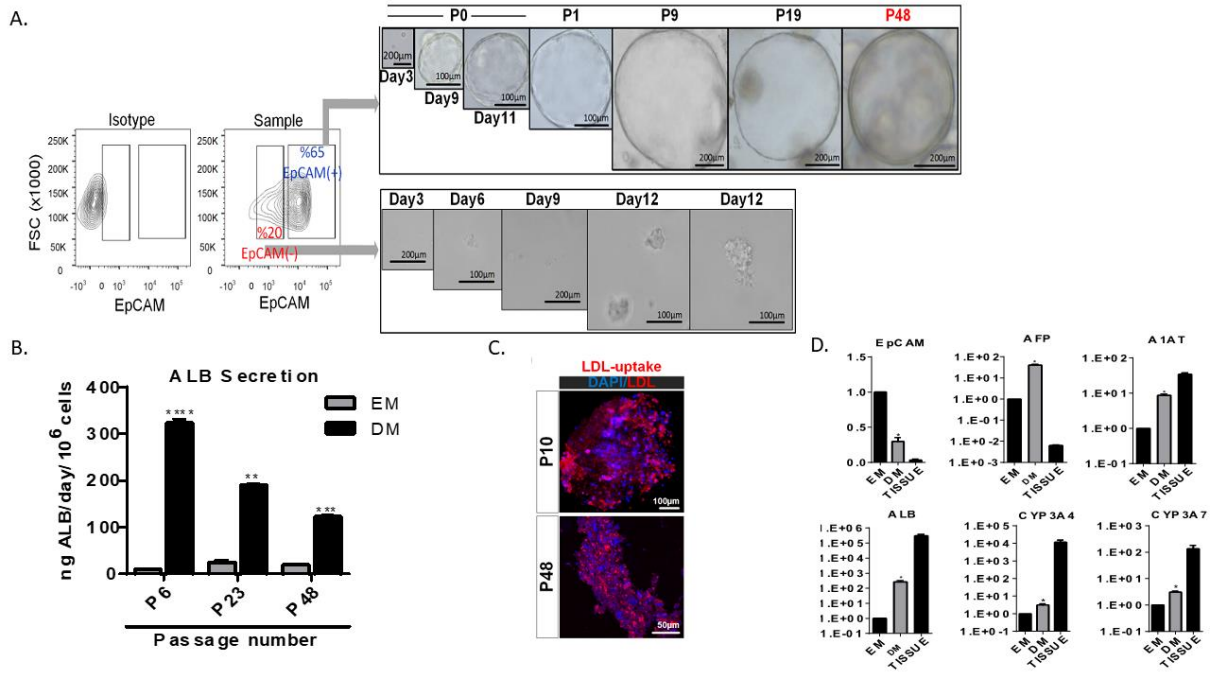


Figure 9: Organoid establishment and functionality tests.

A. FACS gating percentages for the EpCAM+ and EpCAM- cell populations and their efficiency for organoid formation. BF images of organoids at different passages (Left panel). B. Organoid Albumin secretion levels C. LDL-uptake staining of functional eHEPOs D. Gene expression levels for hepatic markers (EM: expansion medium, DM: differentiation medium).

4.2. Determination of LAL Enzyme Activity in Healthy Hepatocytes and eHEPOs

Previous reports by several teams have highlighted the inadequacy of the conventional 2D cultures in terms of representing the function (Boost et al. 2007; Darnell et al. 2012; Kostadinova et al. 2013), therefore we first compared the LAL enzyme activity in the healthy eHEPO samples after 10-14 days of differentiation in comparison with 2D hepatocytes obtained from same iPSC line. The LAL enzyme activity was found to be 7.5 µmol/hour for 2D hepatocytes compared with 58.6 µmol/hour for eHEPOs, showing a significant increase (Figure 10).

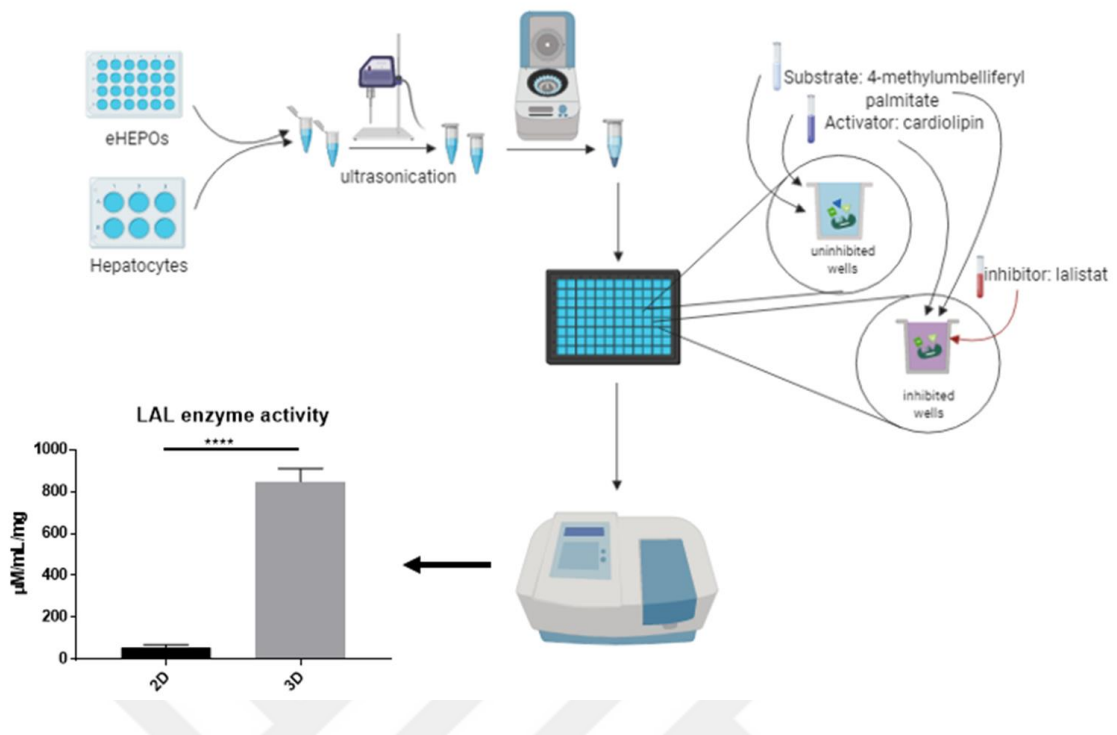


Figure 10: Schematic workflow of the enzyme activity assay and the LAL enzyme activity comparison between 2D hepatocytes and 3D hepatic organoids

The samples are homogenized and centrifuged and enzyme activity reactions are set for inhibited and uninhibited conditions. Spectrophotometric measurements were taken using Varioskan Flash. Specific enzyme activity for both conditions are given in bar graph.

4.3. Determination of Optimal Conditions for Gene Silencing

For the gene silencing an inducible lentiviral shRNA, the system was used. The system has the Tet3G promoter for the expression of shRNA and a constitutive RNA Pol II promoter for the expression of puromycin resistance gene and Tet-On3G transactivator protein. The tet-on3g protein binds to Tet3G promoter only in the presence of doxycycline, thus the shRNA is produced only in the presence of doxycycline. As a negative control, Non-target control (NTC) vector was used, which has the same vector backbone but the shRNA does not target any region in the target organism. Using the system explained above the gene silencing optimizations were done with Huh-7 HCC cell line. First, all 3 shRNA vectors were used to produce viral particles and they were used to transduce Huh-7 cells in combination (shRNA1+shRNA2, shRNA1+shRNA3, shRNA2+shRNA3) or alone (shRNA1, shRNA2, shRNA3). In figure 11A, the workflow of the experiment is schematized. After transduction, the tet-on/off system was induced with doxycycline (1 µg/mL) for 1, 2 and 3 days. GFP expression is observed after 3

days of induction. Meanwhile, to select shRNA expressing cells puromycin (1 $\mu\text{g/mL}$, 2 $\mu\text{g/mL}$, 2.5 $\mu\text{g/mL}$) was added to the culture medium for 3, 5, 7 days. In figure 11B, LIPA gene expression levels of Huh-7 cells after 7 days of 2.5 $\mu\text{g/mL}$ puromycin+ 1 $\mu\text{g/mL}$ doxycycline treatment are seen. All shRNAs except shRNA-3 alone has decreased the expression level of the LIPA gene in Huh7 cell line.

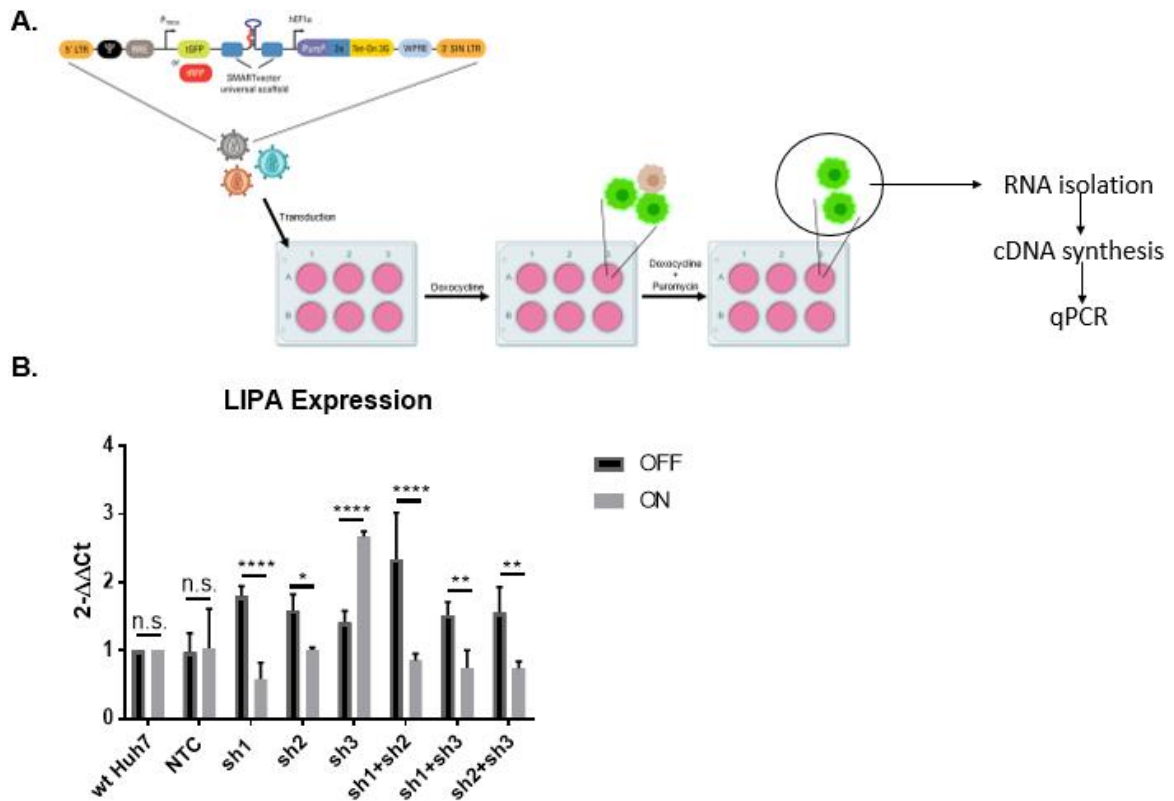


Figure 11: Workflow of the shRNA silencing in Huh-7 cell line and LIPA expression levels after shRNA expression determined via quantitative real-time PCR.

A. Lentiviral particles containing the shRNA sequence are used to transduce the Huh-7 cells, afterwards treatment with doxycycline turns on the inducible system for the expression of both GFP and shRNA. Puromycin selection of the induced system results in GFP⁺ colonies which are then used for RNA isolation and subsequently, gene expression analysis. B. LIPA expression in Huh-7 cells after shRNA silencing is determined via quantitative real-time PCR (ON: shRNA expression is on and LIPA is silenced, OFF: shRNA expression is off and LIPA is not silenced).

4.4. Conditional Knock-Down of LIPA Gene in iPSCs

4.4.1. Establishing LAL Deficient Stable iPSC Lines

Most dramatic silencing effects in Huh-7 cell line were seen with shRNA-1 and combination of shRNA-1 and -2. For the transduction of iPSC colonies, first expression level of LIPA gene in the iPSC cell line was checked. As seen in Figure 12, the relative basal expression level of LIPA in iPSC is 1.18 and HepG2 is 1.9 where the expression level of LIPA in Huh-7 is considered to be 1.

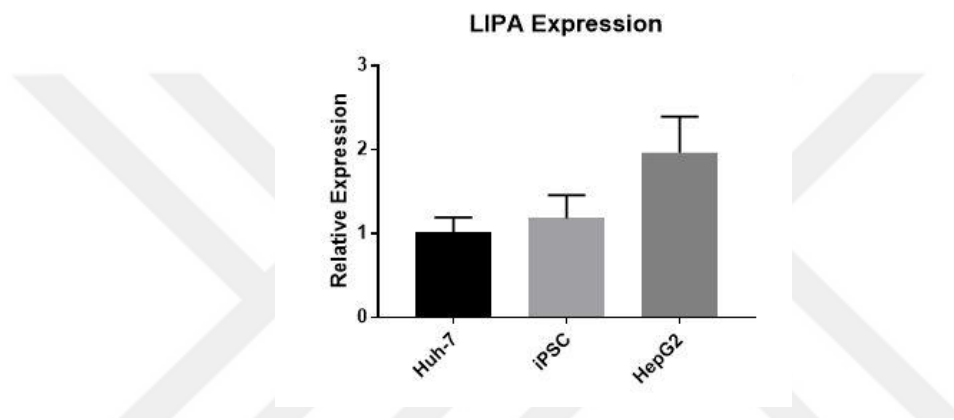


Figure 12: Basal LIPA expression levels in Huh-7, iPSC and HepG2 determined via quantitative real-time PCR.

Huh-7, iPSC and HepG2 mRNA samples were used to detect LIPA expression, shown as relative expression. Normalized with RPL13 as internal control.

After confirming the expression of LIPA in iPSCs, selected 2 shRNA candidates were used for lentiviral transduction. However, 3-day puromycin selection with 1 $\mu\text{g}/\text{mL}$ dose resulted in no viable, undifferentiated colonies. Therefore, all combinations except shRNA-3 were transduced in a new set of wt iPSC colonies. After a 7-day long selection period with puromycin and 1 $\mu\text{g}/\text{ml}$ doxycycline to induce the shRNA system, the silencing percentage of remaining healthy colonies were determined by qPCR, as seen in Figure 13. shRNA-1 and combination of shRNA-1 and -3 has successfully decreased the expression of the LIPA gene by 75% and 70 %, respectively. On the other hand, shRNA-2 did not result in any significant decrease. Other shRNA combinations were lost during the selection process either due to low transfection efficiency or spontaneous differentiation or both. Nevertheless, these 2 conditions (shRNA-1 and combination of shRNA-1 and shRNA-3) were used for the rest of the study.

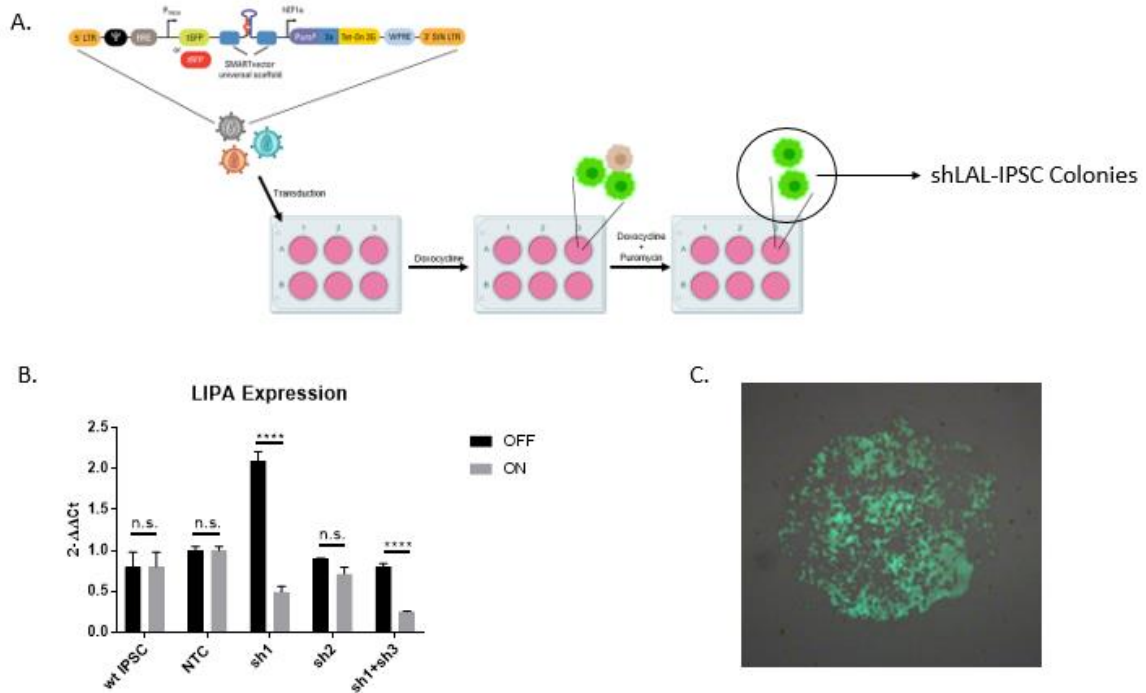


Figure 13: Workflow of the shRNA silencing in iPSC colonies and LIPA expression levels after shRNA expression determined via quantitative real-time PCR.

A. Lentiviral particles containing the shRNA sequence are used to transduce the iPSC colonies, afterwards treatment with doxycycline turns on the inducible system for the expression of both GFP and shRNA. Puromycin selection of the induced system results in GFP+ colonies which are then used for RNA isolation and subsequently, gene expression analysis. B. LIPA expression in iPSC cells after shRNA silencing is determined via quantitative real-time PCR C. Representative image of GFP+ shRNA transfected iPSC colony. (ON: shRNA expression is on and LIPA is silenced, OFF: shRNA expression is off and LIPA is not silenced).

4.4.2. Development of 2D Hepatocyte Culture from LAL Deficient iPSCs

We have used the protocol of Chen and his colleagues to obtain healthy 2D hepatocyte cultures (Chen et al. 2012). These hepatocytes are shown to have hepatic functions such as albumin secretion and expression of hepatocyte-specific genes as determined earlier (Akbari S., unpublished data). After stably transfecting the iPSC colonies the same differentiation protocol was used to obtain LAL-deficient hepatocyte cultures. In Figure 14, bright field images at the different stages of the differentiation procedure for wt, NTC and LAL deficient colonies are shown.

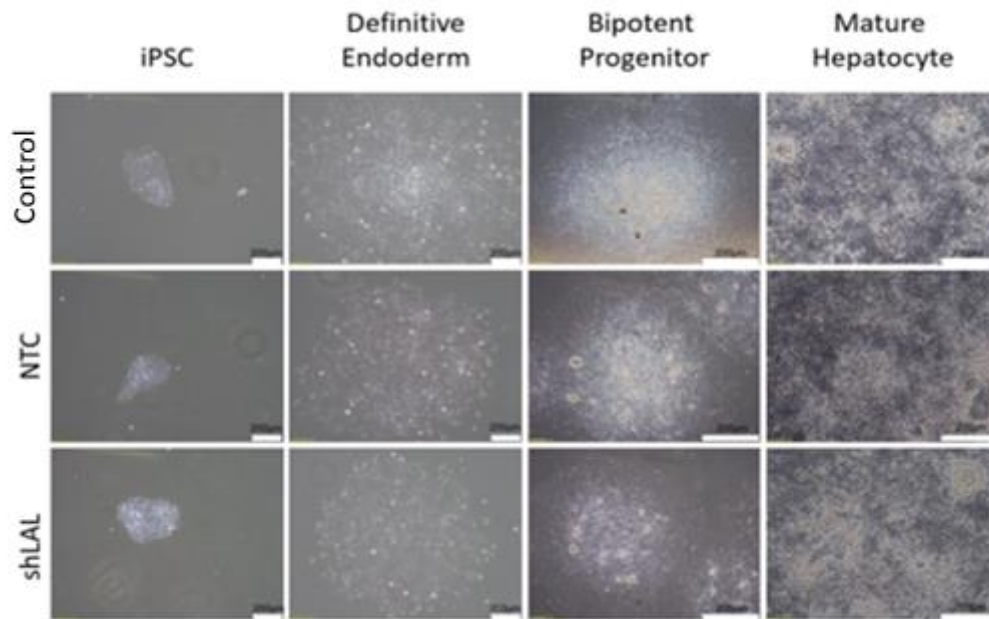


Figure 14: BF images of differentiated iPSC colonies

Wt iPSC, DE, BP and MH cells under BF microscope (Top). NTC vector transduced iPSC, DE, BP and MH cells under BF microscope (middle). shRNA-1 transduced iPSC, DE, BP and MH cells under BF microscope (bottom). Scale bar: 200 μ m.

4.4.3. Development of 3D Hepatocyte Culture from LAL Deficient iPSCs

Colonies of shLAL and NTC produced in the previous steps were differentiated to DE with a 5-day induction with Activin-A. During this process, cells were also induced with doxycycline to induce GFP and shRNA expression. Then the cells expressing both GFP and EpCAM are sorted to establish eHEPO cultures (Figure 15).

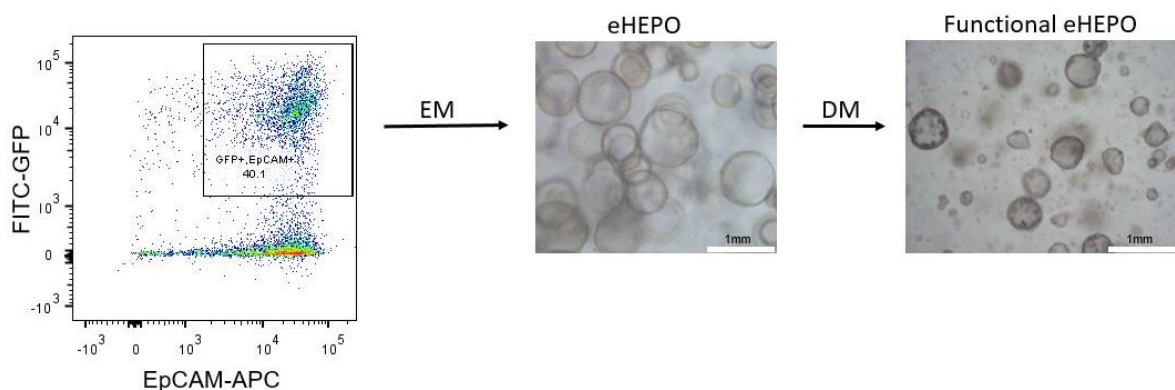


Figure 15: FACS gating percentage for the EpCAM+/GFP+ cell population and BF images of EM and DM eHEPOs.

DE cells were sorted for EpCAM+/GFP+ double positivity and embedded in matrigel to form eHEPOs.

4.4. Verification of 2D and 3D LALD Model

The eHEPOs were serially passaged to expand and then differentiated in DM for 10-14 days for the LAL enzyme activity assay. The specific enzyme activity is calculated with the following equation: Enzyme activity (μM) / protein concentration (mg/mL). Accordingly, the specific LAL enzyme activity of NTC eHEPOs is $96 \mu\text{M}/\text{mL}/\text{mg}$ and $100 \mu\text{M}/\text{mL}/\text{mg}$ for shRNA1-3 transfected but not induced eHEPOs while it is $156 \mu\text{M}/\text{mL}/\text{mg}$ for LAL deficient eHEPOs (LeHEPOs) demonstrating an enzyme activity increase in the LAL deficient group as seen in Figure 16.

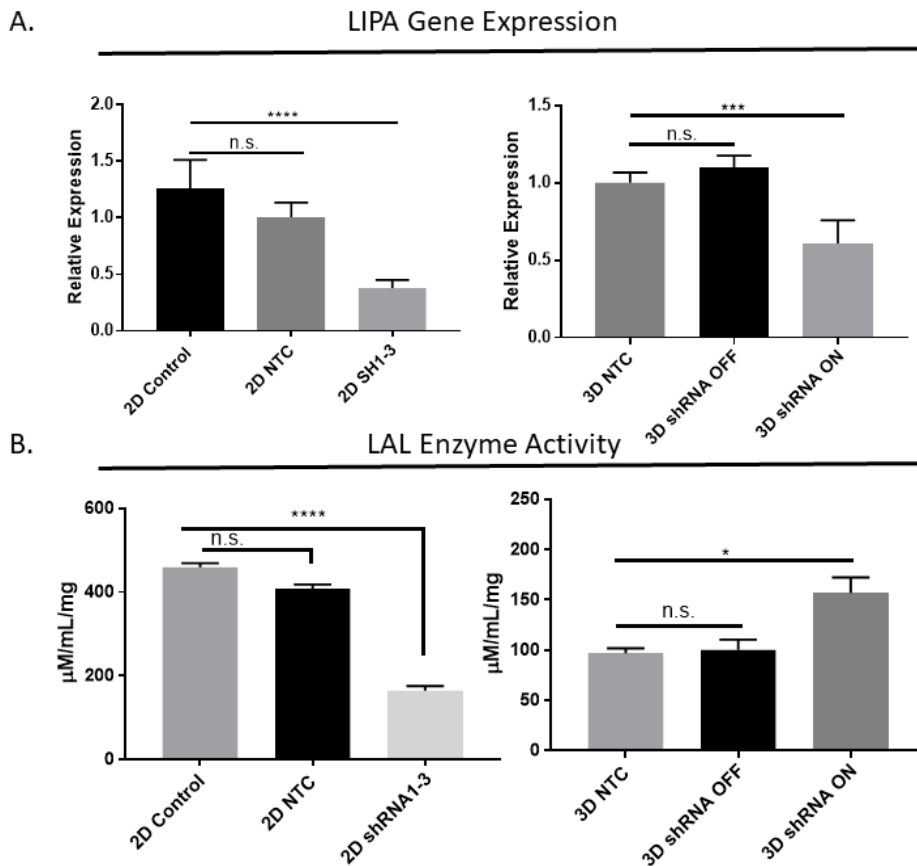


Figure 16: LIPA gene expression levels of differentiated 2D and 3D hepatocytes and determination of specific activity of the LAL enzyme

A. LIPA gene expression levels of differentiated 2D and 3D hepatocytes represented as relative expression.
B. Specific activity of the LAL enzyme in WT and LALD hepatocytes and eHEPOs measured by spectrophotometry.

2D hepatocytes differentiated from iPSCs, however, have the following LAL enzyme activity levels: 459 and 408 $\mu\text{M}/\text{mL}/\text{mg}$ for the WT and NTC samples. Importantly, specific enzyme activity is significantly less in shLAL1-3 sample with 164 $\mu\text{M}/\text{mL}/\text{mg}$ (Figure 16).

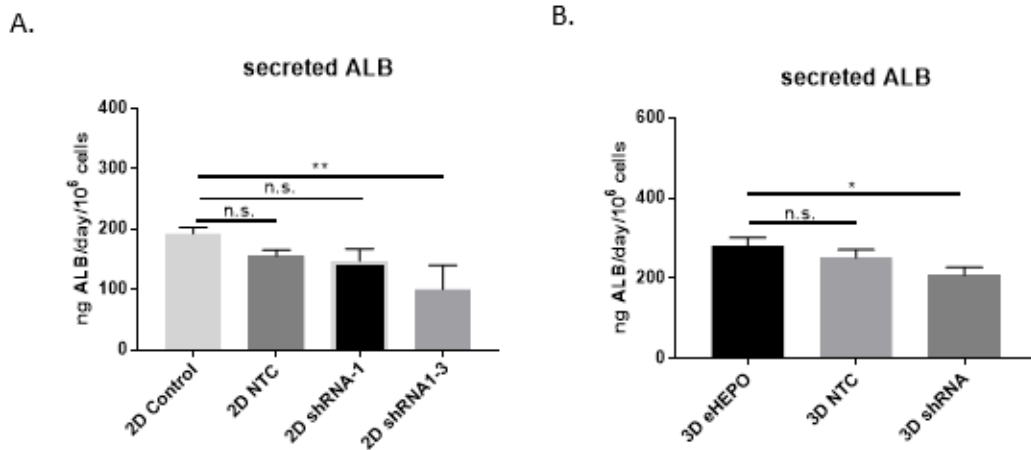


Figure 17: Albumin secretion levels of 2D and 3D models are determined by ELISA.

A. Secreted albumin levels of 2D WT, NTC and LAL deficient hepatocytes. B. Secreted albumin levels of 3D WT, NTC and LAL deficient hepatic organoids. EM is for eHEPO and DM is for differentiated, functional eHEPO.

To assess whether this LIPA silencing has caused other expressional and functional changes in these models albumin secretion, lipid accumulation, and gene expression analysis were performed. Both differentiated eHEPOs and 2D hepatocytes were capable of albumin secretion and the albumin levels of 2D hepatocytes were comparable to each other with 192, 155 and, 147 ng/day/10⁶ for WT and NTC respectively. Interestingly, shRNA1-3 transduced hepatocytes had a significantly lower level of secreted albumin with 100 ng/day/10⁶. Similarly, WT and NTC eHEPOs secreted 281 ng/day/10⁶ and 250 ng/day/10⁶ albumin. However, the albumin level of LeHEPOs was slightly reduced with 207 ng/day/10⁶ (Figure 17).

Further assessment of the hepatic functions in the models was performed with lipid staining. As previously explained, LALD causes excessive lipid accumulation in the hepatocytes. To be able to observe the difference more dramatically, cells were incubated with 50 μM serum cholesterol-containing medium one day prior to staining. As seen in Figure 18, the immunofluorescent signal coming from WT hepatocytes is less than that of LAL deficient hepatocytes. On the contrary, whole-mount stainings of WT and LAL deficient eHEPOs does not seem to differ much (Figure 18).

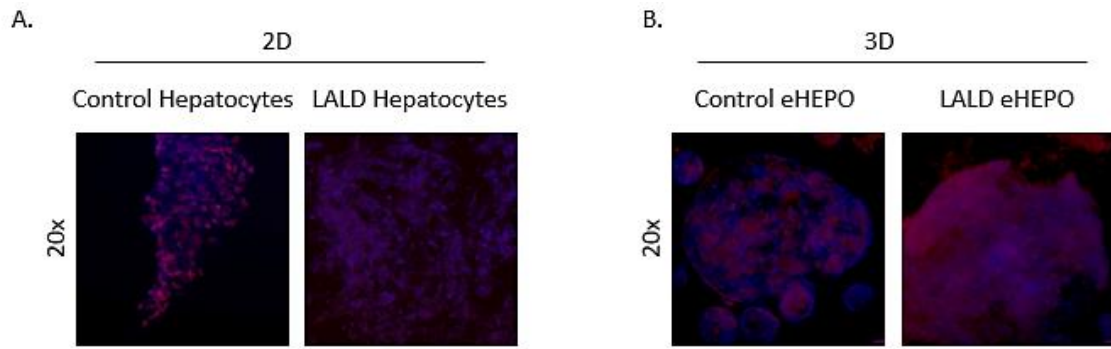


Figure 18: Immunofluorescent staining of 2D and 3D hepatocytes (MDH: lipid, PI: nucleus)



5. DISCUSSION

Organoid models with long term expansion ability and benefits of resembling the disease pathology have made them amenable choices for disease modeling. Especially, the modeling of genetic diseases has been valuable for the exploration of new therapeutic approaches. Patient-derived intestinal organoids for cystic fibrosis (CF) modeling has been successfully produced by Beekman and co-workers in 2013. CF is caused by mutations in the cystic fibrosis transmembrane conductance regulator (CFTR) gene, coding for a membrane channel protein. In the case of the mutated CFTR gene, the defective protein leads to the excessive accumulation of viscous mucosal secretions in both respiratory and gastrointestinal tract. The model has successfully been used for the prediction of effective drugs for different mutations (Dekkers et al., 2013). Another successful organoid model for a genetic disease is for the α 1-antitrypsin (A1AT) deficiency. Again, mutations in the gene for A1AT causes defective protein folding, eventually leading to chronic liver failure. Patient-derived liver organoids for A1AT deficiency has been established by Huch and co-workers (Huch et al., 2015), and similarly, a patient-derived organoid model of the citrullinemia disease have been created by our team (Akbari et al., under revision). These models have been successful to show the disease phenotype *in vitro* and provided a tool for further investigation of potential therapeutics.

Similarly, our aim was to create an organoid model for the LALD using a slightly different approach. Our model is based on inducible silencing of the LIPA gene since the stable knock-out / complete knock-down of the gene leads to severely uncompromised hepatocytes and would be very challenging to expand long-term. During this process, we have also produced LAL deficient 2D hepatocytes to compare the efficiency of our system. Since 2D cultures are shown to be less effective in the regulation of metabolic functions (Boost et al. 2007; Darnell et al. 2012; Kostadinova et al. 2013) the regulation of enzyme activity is not as tightly controlled as 3D. Therefore, a 70% decrease in the gene expression of 2D hepatocytes can lead to a significant change in the enzyme activity. However, that is not the case for LALD patients. In order to see the phenotype in humans, the gene expression of LIPA needs to be less than 5%. Since our knock-down of LIPA gene is not as dramatic (only 40% decrease), we could not be able to observe any decrease in enzyme activity. On the contrary, we have observed an increase that could be simply due to a technical issue about 3D culture materials interfering with enzyme

activity or leading to incomplete homogenization during enzyme activity assay procedure. Technical insufficiencies of the protocol need to be improved before a further investigation of the system is performed. Moreover, lipid staining after 24-hour cholesterol induction has shown an increase in the intensity of lipid stainings of 2D culture system whereas 3D culture has shown similar staining intensities. The whole-mount stainings of 3D systems are tricky to identify a meaningful difference. Usage of a quantitative method or improving the staining method by using either organoid cross-sections or changing the dye can provide a better understanding of the conditions. A more detailed investigation for the optimization of 3D culture would clarify this issue. Of note, a very recent study by Takebe and co-workers have announced the patient-derived organoid model of WD in the last month. In this work, the team uses WD patient iPSCs to establish hepatic organoids and consequently model hepatic steatohepatitis. Importantly, they also utilize this model for investigation of a therapeutic agent to rescue the disease phenotype.

To sum up, our 2D model has been successful to exhibit the disease phenotype but the long-term expansion of these systems are not efficient. Also, since the regulation of enzyme activity is not as tightly controlled as 3D system, a 2D model would not be as reliable. Hence, the improvements for the 3D model will be implemented to obtain a higher degree of gene silencing to be able to see the phenotypic effect.

6. CONCLUSION AND FUTURE ASPECTS

We have successfully developed a 2D hepatic LALD model with inducible shRNA silencing of the LIPA gene. However, our 3D model is needed to be improved to see phenotype of the disease. The methods for the enzyme activity detection is established and optimized for cells of 2D culture. Preliminary work to optimize the 3D culture enzyme activity has proven the importance of the volume of starting material. Since the proliferation rate and organoid formation efficiency of 3D culture are effected after gene silencing, starting material volume for the enzyme activity was not equal for all samples, this leads to the uncomplete homogenization of the samples which results in lower enzyme activity levels even though total protein amount is higher. This technical issues about our experimental set-up will be improved for future work.

Previously established hepatic organoid model of WD have been reported to have a compromised survival ability due to enzyme deficiency but in our model LAL silencing can be turned off for the expansion and long term culture of the organoids. Moreover, the lentiviral shRNA vector system provides the possibility of varying levels of gene silencing. This could be used to investigate the effects of mildly reduced LAL activity at the molecular level even if the disease phenotype is not seen. However, our model could be improved by creating LAL deficient iPCS lines and transfecting them with mutated LIPA sequence containing inducible vectors. Thus, the system would represent the known mutations of patients and still have the benefit of an inducible system. In addition, our study needs a deeper investigation of hepatic functions of the disease model, i.e.: CYP activity, glycogen storage ability, LDL uptake ability, and hepatocyte-specific gene expressions should have been checked. Gene expression levels of glucose and lipid metabolism-related pathways could have been screened to investigate alterations of these pathways.

7. REFERENCES

- Aguisanda, Francis et al. 2017. “Neural Stem Cells for Disease Modeling of Wolman Disease and Evaluation of Therapeutics.” *Orphanet Journal of Rare Diseases* 12(1): 1–13.
- Baxter, Melissa et al. 2015. “Phenotypic and Functional Analyses Show Stem Cell-Derived Hepatocyte-like Cells Better Mimic Fetal Rather than Adult Hepatocytes.” *Journal of Hepatology* 62(3): 581–89. <http://dx.doi.org/10.1016/j.jhep.2014.10.016>.
- Berasain, Carmen, and Matías A. Avila. 2015. “Regulation of Hepatocyte Identity and Quiescence.” *Cellular and Molecular Life Sciences* 72(20): 3831–51.
- van den Berg, Cathelijne W. et al. 2018. “Renal Subcapsular Transplantation of PSC-Derived Kidney Organoids Induces Neo-Vasculogenesis and Significant Glomerular and Tubular Maturation In Vivo.” *Stem Cell Reports* 10(3): 751–65.
- Bernstein, Donna L., Helena Hülkova, Martin G. Bialer, and Robert J. Desnick. 2013. “Cholesteryl Ester Storage Disease: Review of the Findings in 135 Reported Patients with an Underdiagnosed Disease.” *Journal of Hepatology* 58(6): 1230–43. <http://dx.doi.org/10.1016/j.jhep.2013.02.014>.
- Bissell, D. M., D. M. Arenson, J. J. Maher, and F. J. Roll. 1987. “Support of Cultured Hepatocytes by a Laminin-Rich Gel. Evidence for a Functionally Significant Subendothelial Matrix in Normal Rat Liver.” *Journal of Clinical Investigation* 79(3): 801–12.
- Boost, Kim A. et al. 2007. “Long-Term Production of Major Coagulation Factors and Inhibitors by Primary Human Hepatocytes in Vitro: Perspectives for Clinical Application.” *Liver International* 27(6): 832–44.
- Carter, Anna, Simon Mark Brackley, Jiali Gao, and Jake Peter Mann. 2019. “The Global Prevalence and Genetic Spectrum of Lysosomal Acid Lipase Deficiency: A Rare Condition That Mimics NAFLD.” *Journal of Hepatology* 70(1): 142–50. <https://doi.org/10.1016/j.jhep.2018.09.028>.
- Chen, Yu Fan et al. 2012. “Rapid Generation of Mature Hepatocyte-like Cells from Human Induced Pluripotent Stem Cells by an Efficient Three-Step Protocol.” *Hepatology* 55(4): 1193–1203.
- Clayton, D F, and J E Darnell. 2015. “Changes in Liver-Specific Compared to Common Gene Transcription during Primary Culture of Mouse Hepatocytes.” *Molecular and Cellular*

- Biology* 3(9): 1552–61.
- Clevers, Hans. 2016. “Modeling Development and Disease with Organoids.” *Cell* 165(7): 1586–97. <http://dx.doi.org/10.1016/j.cell.2016.05.082>.
- Darnell, M. et al. 2012. “In Vitro Evaluation of Major In Vivo Drug Metabolic Pathways Using Primary Human Hepatocytes and HepaRG Cells in Suspension and a Dynamic Three-Dimensional Bioreactor System.” *Journal of Pharmacology and Experimental Therapeutics* 343(1): 134–44.
- Du, H. et al., 2001. “Enzyme Therapy for Lysosomal Acid Lipase Deficiency in the Mouse.” *Human Molecular Genetics* 10(16): 1639–48.
- Du, H. et al., 2002. “Lysosomal Acid Lipase Deficiency: Correction of Lipid Storage by Adenovirus-Mediated Gene Transfer in Mice.” *Human Gene Therapy* 13(11): 1361–72.
- Du, H. et al., 2005. “The Role of Mannosylated Enzyme and the Mannose Receptor in Enzyme Replacement Therapy.” *The American Journal of Human Genetics* 77(6): 1061–74.
- Du, H. et al., 2008. “Wolman Disease/Cholesteryl Ester Storage Disease: Efficacy of Plant-Produced Human Lysosomal Acid Lipase in Mice.” *Journal of Lipid Research* 49(8): 1646–57.
- Du, Hong, Ming Duanmu, David Witte, and Gregory A. Grabowski. 1998. “Targeted Disruption of the Mouse Lysosomal Acid Lipase Gene: Long-Term Survival with Massive Cholesteryl Ester and Triglyceride Storage.” *Human Molecular Genetics* 7(9): 1347–54.
- Dubland, Joshua A., and Gordon A. Francis. 2015. “Lysosomal Acid Lipase: At the Crossroads of Normal and Atherogenic Cholesterol Metabolism.” *Frontiers in Cell and Developmental Biology* 3(February): 1–11.
- Duval, Kayla et al. 2017. “Modeling Physiological Events in 2D vs. 3D Cell Culture.” *Physiology* 32(4): 266–77. <http://www.physiology.org/doi/10.1152/physiol.00036.2016>.
- Frampton, James E. 2016. “Sebelipase Alfa: A Review in Lysosomal Acid Lipase Deficiency.” *American Journal of Cardiovascular Drugs* 16(6): 461–68.
- Gordillo, M., T. Evans, and V. Gouon-Evans. 2015. “Orchestrating Liver Development.” *Development* 142(12): 2094–2108. <http://dev.biologists.org/cgi/doi/10.1242/dev.114215>.
- Guan, Yuan et al. 2017. “Human Hepatic Organoids for the Analysis of Human Genetic Diseases.” 2(17): 1–17. <https://doi.org/10.1172/jci.insight.94954>.
- Hua, Liu et al. 2011. “In Vivo Liver Regeneration Potential of Human Induced Pluripotent Stem Cells from Diverse Origins.” *Science translational medicine* 3(82): 82ra39.

- <http://stm.sciencemag.org/content/3/82/82ra39.short>.
- Huch, Meritxell et al. 2013. “In Vitro Expansion of Single Lgr5 + Liver Stem Cells Induced by Wnt-Driven Regeneration.” *Nature* 494(7436): 247–50. <http://dx.doi.org/10.1038/nature11826>.
- Huch, Meritxell et al., 2015. “Long-Term Culture of Genome-Stable Bipotent Stem Cells from Adult Human Liver.” *Cell* 160(1–2): 299–312. <http://dx.doi.org/10.1016/j.cell.2014.11.050>.
- Kostadinova, Radina et al. 2013. “A Long-Term Three Dimensional Liver Co-Culture System for Improved Prediction of Clinically Relevant Drug-Induced Hepatotoxicity.” *Toxicology and Applied Pharmacology* 268(1): 1–16. <http://dx.doi.org/10.1016/j.taap.2013.01.012>.
- Kuriwaki, Kazumi, and Hiroki Yoshida. 1999. “Morphological Characteristics of Lipid Accumulation in Liver- Constituting Cells of Acid Lipase Deficiency Rats (Wolman’s Disease Model Rats).” *Pathology International* 49(4): 291–97.
- Kuriyama Masaru, Yoshida Hiroki, Suzuki Minoru, Fujiyama Jiro and Igata Akihiro. 1990. “Lysosomal Acid Lipase Deficiency in Rats: Lipid Analyses and Lipase Activities in Liver and Spleen.” *Journal of Lipid Research* 31(9): 1605–12.
- Li, Fang, and Hanrui Zhang. 2019. “Lysosomal Acid Lipase in Lipid Metabolism and Beyond.” *Arteriosclerosis, thrombosis, and vascular biology* 39(5): 850–56.
- Liangyou, Rui. 2014. “Energy Metabolism in the Liver.” *Compr Physiol.* 4(1): 177–97.
- Lu, Wenqi et al. 2017. “Crypt Organoid Culture as an in Vitro Model in Drug Metabolism and Cytotoxicity Studies.” *Drug Metabolism and Disposition* 45(7): 748–54.
- Meli, Luciana et al. 2012. “Influence of a Three-Dimensional, Microarray Environment on Human Cell Culture in Drug Screening Systems.” *Biomaterials* 33(35): 9087–96. <http://dx.doi.org/10.1016/j.biomaterials.2012.08.065>.
- Mitaka, Toshihiro, and Hidekazu Ooe. 2010. “Characterization of Hepatic-Organoid Cultures.” *Drug Metabolism Reviews* 42(3): 472–81.
- Ouchi, Rie et al. 2019. “Modeling Steatohepatitis in Humans with Pluripotent Stem Cell-Derived Organoids.” *Cell Metabolism* 30: 1–11. <https://linkinghub.elsevier.com/retrieve/pii/S1550413119302475>.
- Radović, Branislav et al. 2016. “Lysosomal Acid Lipase Regulates VLDL Synthesis and Insulin Sensitivity in Mice.” *Diabetologia* 59(8): 1743–52.
- Reiner, Željko et al. 2014. “Lysosomal Acid Lipase Deficiency - An under-Recognized Cause

- of Dyslipidaemia and Liver Dysfunction.” *Atherosclerosis* 235(1): 21–30.
- Rowe, R. Grant, and George Q. Daley. 2019. “Induced Pluripotent Stem Cells in Disease Modelling and Drug Discovery.” *Nature Reviews Genetics*. <http://dx.doi.org/10.1038/s41576-019-0100-z>.
- Si-Tayeb, Karim et al. 2010. “Highly Efficient Generation of Human Hepatocyte-like Cells from Induced Pluripotent Stem Cells.” *Hepatology* 51(1): 297–305.
- Sun, Ying et al. 2014. “Reversal of Advanced Disease in Lysosomal Acid Lipase Deficient Mice: A Model for Lysosomal Acid Lipase Deficiency Disease.” *Molecular Genetics and Metabolism* 112(3): 229–41. <http://dx.doi.org/10.1016/j.ymgme.2014.04.006>.
- Takahashi Kazutoshi, Tanabe Koji, Ohnuki Mari, Narita Megumi, Ichisaka Tomoko, Tomoda Kiichiro, Yamanaka Shinya. 2007. “Induction of Pluripotent Stem Cells from Adult Human Fibroblasts by Defined Factors.” *Cell* 131: 861–72.
- Takebe, Takanori et al. 2013. “Vascularized and Functional Human Liver from an iPSC-Derived Organ Bud Transplant.” *Nature* 499(7459): 481–84. <http://dx.doi.org/10.1038/nature12271>.
- Thelwall, Peter E. et al. 2013. “Hepatic Cholesteryl Ester Accumulation in Lysosomal Acid Lipase Deficiency: Non-Invasive Identification and Treatment Monitoring by Magnetic Resonance.” *Journal of Hepatology* 59(3): 543–49.
- Wang, Helen H. et al. 2017. “Cholesterol and Lipoprotein Metabolism and Atherosclerosis: Recent Advances in Reverse Cholesterol Transport.” *Annals of Hepatology* 16: s27–42. <http://dx.doi.org/10.5604/01.3001.0010.5495>.
- Watanabe, Momoko et al. 2017. “Self-Organized Cerebral Organoids with Human-Specific Features Predict Effective Drugs to Combat Zika Virus Infection.” *Cell Reports* 21(2): 517–32. <https://doi.org/10.1016/j.celrep.2017.09.047>.
- Wu, Haojia et al. 2018. “Comparative Analysis and Refinement of Human PSC-Derived Kidney Organoid Differentiation with Single-Cell Transcriptomics.” *Cell Stem Cell* 23(6): 869–881.e8. <https://doi.org/10.1016/j.stem.2018.10.010>.